

RICE UNIVERSITY

Magnetic Damping of an Elastic Conductor

by

Jeffrey M. Hokanson

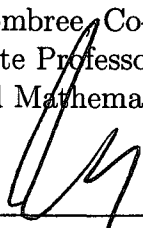
A THESIS SUBMITTED
IN PARTIAL FULFILLMENT OF THE
REQUIREMENTS FOR THE DEGREE

Master of Arts

APPROVED, THESIS COMMITTEE:



Mark Embree, Co-chair
Associate Professor of Computational and
Applied Mathematics



Steven J. Cox, Co-chair
Professor of Computational and Applied
Mathematics



David Damanik
Associate Professor of Mathematics

Houston, Texas

April, 2009

UMI Number: 1466785

INFORMATION TO USERS

The quality of this reproduction is dependent upon the quality of the copy submitted. Broken or indistinct print, colored or poor quality illustrations and photographs, print bleed-through, substandard margins, and improper alignment can adversely affect reproduction.

In the unlikely event that the author did not send a complete manuscript and there are missing pages, these will be noted. Also, if unauthorized copyright material had to be removed, a note will indicate the deletion.

UMI[®]

UMI Microform 1466785

Copyright 2009 by ProQuest LLC

All rights reserved. This microform edition is protected against unauthorized copying under Title 17, United States Code.

ProQuest LLC
789 East Eisenhower Parkway
P.O. Box 1346
Ann Arbor, MI 48106-1346

ABSTRACT

Magnetic Damping of an Elastic Conductor

by

Jeffrey M. Hokanson

Many applications call for a design that maximizes the rate of energy decay. Typical problems of this class include one dimensional damped wave operators, where energy dissipation is caused by a damping operator acting on the velocity. Two damping operators are well understood: a multiplication operator (known as viscous damping) and a scaled Laplacian (known as Kelvin–Voigt damping). Paralleling the analysis of viscous damping, this thesis investigates energy decay for a novel third operator known as magnetic damping, where the damping is expressed via a rank-one self-adjoint operator, dependent on a function a . This operator describes a conductive monochord embedded in a spatially varying magnetic field perpendicular to the monochord and proportional to a . Through an analysis of the spectrum, this thesis suggests that unless a has a singularity at one boundary for any finite time, there exist initial conditions that give arbitrarily small energy decay at any time.

Contents

| | |
|--|-----------|
| List of Illustrations | v |
| List of Tables | vi |
| 1 Introduction | 1 |
| 2 A Menagerie of Wave Operators | 5 |
| 2.1 Undamped wave operator | 6 |
| 2.2 Kelvin–Voigt damping | 7 |
| 2.3 Viscous damping | 8 |
| 2.4 Magnetic damping | 13 |
| 3 Basic Results for Magnetic Damping | 16 |
| 3.1 Explicit form for the resolvent | 17 |
| 3.1.1 Inverting $A - \lambda$ via triangular factorization | 17 |
| 3.1.2 Green’s function | 19 |
| 3.2 Discrete spectra | 19 |
| 3.3 Shooting function | 25 |
| 4 Bounded Variation Fields | 27 |
| 4.1 Spectral abscissa for bounded variation a | 27 |
| 4.2 Bounds on the spectrum | 29 |
| 4.3 Resolvent bound in terms of Fourier coefficients | 32 |
| 4.4 A sinusoidal damping field | 33 |
| 4.5 Finite bandwidth a | 35 |
| 5 Singular Damping Fields | 37 |
| 5.1 Rate of leaving the axis | 37 |
| 5.1.1 Example when $a(x) = \gamma/x$ | 39 |
| 5.2 Resolvent upper bound | 40 |
| 5.3 Resolvent lower bound | 42 |
| 5.4 Is $a(x) = \gamma/x$ optimal? | 46 |
| 6 Conclusions | 48 |
| A Derivation of Magnetic Damping | 50 |

| | |
|---|---------------|
| B Spectral Methods | 54 |
| B.1 Chebyshev differentiation matrices | 54 |
| B.2 Approximating the undamped wave operator | 55 |
| B.3 Approximating the magnetic damping operator | 57 |
| Bibliography | 61 |

Illustrations

| | | |
|-----|---|----|
| 2.1 | Spectrum of the Kelvin–Voigt damping with constant $a(x) \equiv \gamma = 2/5$. | 9 |
| 2.2 | Spectrum of the viscous damping operator with constant $a(x) \equiv \gamma = 2$. | 11 |
| 2.3 | Spectrum of the magnetic damping operator with constant $a(x) \equiv \gamma = 0.8745$ | 15 |
| 3.1 | Green’s function for $a(x) = 1$ | 20 |
| 4.1 | Bounds provided by Theorem 5 | 31 |
| 4.2 | Eigenvalues of A when $a(x) = \gamma\phi_2(x)$ | 34 |
| 5.1 | Upper bound on the resolvent for a singular field | 43 |
| 5.2 | Mollification lower bound on the resolvent | 45 |
| 5.3 | Spectrum of A when $a(x) = 2/(\pi x)$ | 46 |
| A.1 | Physical setting for magnetic damping | 51 |
| B.1 | Code generating an approximation of the undamped wave operator. . | 57 |
| B.2 | Code generating an approximation of the magnetic damping operator. . | 59 |

Tables

| | | |
|-----|--|----|
| 5.1 | Illustration of Theorem 7 | 40 |
| 5.2 | Numerically optimal finite Laurent series | 47 |
| A.1 | Variables required for derivation of magnetic damping equations of motion | 51 |
| B.1 | Convergence of spectral methods for the undamped wave operator . . | 56 |
| B.2 | Eigenvalue convergence for spectral approximation of the magnetic damping operator when $a \in BV(0, \pi)$ | 59 |
| B.3 | Eigenvalue convergence for spectral approximation of the magnetic damping operator when $a(x) = 2/(\pi x)$ | 60 |

Chapter 1

Introduction

Minimization of energy is a common design objective for physical systems. Frequently, engineers attempt to design systems such that the energy introduced by perturbations is quickly removed. For example, a car designer might want a door to close silently. A key strategy problem would then be to place damping material in the door to maximize the rate of energy decay. Design problems such as these motivate the study of damped wave operators, which manifest many characteristics of harder problems yet yield to rigorous analysis. Two of these operators have been subjected to thorough study: the Kelvin–Voigt and viscous damping operators. In this thesis I analyze a novel third damped wave operator associated with magnetic damping to find the conditions for maximizing energy decay.

Magnetic damping was first studied by Leibowitz and Ackerberg in 1963 [14]. After rescaling variables, they found that a conductive string embedded in a magnetic field string obeyed the integro-differential equation

$$\frac{\partial^2 u}{\partial t^2} - \frac{\partial^2 u}{\partial x^2} = -a(x) \int_0^\pi a(\xi) \frac{\partial}{\partial t} u(\xi, t) d\xi \quad (1.1)$$

$$u(0, t) = u(\pi, t) = 0,$$

where $u(x, t)$ measures transverse displacement and $a(x)$ is proportional to the magnetic field intensity. A derivation of the equations of motion is given in Appendix A. In this thesis I demonstrate how the choice of a affects the rate of energy decay.

Magnetic damping can be understood in a similar manner to other damped wave

operators. Following the approach of Cox and Zuazua [7] for viscous damping, I study energy decay by converting the second order partial differential equation (1.1) into the first order form

$$\frac{\partial}{\partial t} \begin{bmatrix} u \\ \frac{\partial u}{\partial t} \end{bmatrix} = A \begin{bmatrix} u \\ \frac{\partial u}{\partial t} \end{bmatrix},$$

where A is an operator posed on a space X endowed with an inner product measuring system energy. Under these conditions the spectrum of A reveals energy decay properties. For magnetic damping, A takes the form

$$A = \begin{bmatrix} 0 & I \\ \Delta & -a\langle \cdot, a \rangle \end{bmatrix}. \quad (1.2)$$

Here and for the remainder of this thesis, $\langle \cdot, \cdot \rangle$ is the standard $L^2(0, \pi)$ inner product

$$\langle f, g \rangle = \int_0^\pi f(x) \overline{g(x)} dx.$$

Similarly, the $L^2(0, \pi)$ norm is denoted $\| \cdot \|$, where $\|f\| = \langle f, f \rangle^{1/2}$. The operator A is posed on the space $X = H_0^1(0, \pi) \times L^2(0, \pi)$ with energy inner product

$$\langle [u, v]^T, [f, g]^T \rangle_X = \int_0^\pi u'(x) \overline{f'(x)} dx + \int_0^\pi v(x) \overline{g(x)} dx \quad (1.3)$$

and norm $\|V\|_X = \langle V, V \rangle_X^{1/2}$. The norm $\| \cdot \|_X$ is a measure of the total energy in the string: the first term in (1.3) measures potential energy; the second kinetic. Let $L(X)$ denote the set of bounded linear operators on X . For $T \in L(X)$ the energy norm induces the operator norm

$$\|T\|_{L(X)} = \sup_{\|V\|_X=1} \|TV\|_X.$$

The operator A maps

$$\text{Dom}(A) = \{[u, v]^T \in H_0^1(0, \pi) \times L^2(0, \pi) : u'' - a\langle v, a \rangle \in L^2(0, \pi)\}$$

to X . This operator also generates a C_0 semigroup; thus for an initial condition $V_0 \in X$, the energy in the system is written as

$$\mathcal{E}(t) = \|e^{tA}V_0\|_X^2.$$

(Here we understand e^{tA} in the sense of [22, §15].) The asymptotic rate of energy decay, $\omega(A)$, is the smallest scalar such that

$$\mathcal{E}(t) \leq \|e^{tA}\|_{L(X)}^2 \|V_0\|_X^2 \leq Ce^{t2\omega(A)} \quad (1.4)$$

for some $C > 0$ and for all $V_0 \in \text{Dom}(A)$. Let $\sigma(A)$ denote the spectrum of A , that is, the set of all $\lambda \in \mathbb{C}$ such that $A - \lambda$ does not have a bounded, densely defined inverse. The spectral abscissa,

$$\alpha(A) = \sup_{\lambda \in \sigma(A)} \text{Re}(\lambda),$$

is always a lower bound on energy decay: $\alpha(A) \leq \omega(A)$. Under certain restrictions on A , the reverse inequality can be shown, and thus $\alpha(A) = \omega(A)$. Theorem 4 in chapter 4 will show that if a is a function of bounded variation, $a \in BV(0, \pi)$, then $\alpha(A) = \omega(A)$. Further, when $a \in BV(0, \pi)$, Theorem 3 demonstrates that $\alpha(A) = 0$. Thus for bounded variation magnetic fields at any finite time τ , there exists initial conditions that manifest arbitrarily small energy decay at $t = \tau$. The lack of energy decay will motivate my study of singular fields in chapter 5, i.e., those a for which there exist constants $C > 0$ and $p > -3/2$ such that

$$|a(x)| \leq Cx^p(\pi - x)^p$$

for all $x \in (0, \pi)$. Even when a is singular, the spectrum of A still contains only eigenvalues, as demonstrated in Theorem 1 in chapter 3. Analysis and computations for such singular damping are considerably complicated by the unbounded nature of

a. No proofs establishing $\alpha(A) = \omega(A)$ are demonstrated here for singular fields, nor any results establishing $\alpha(A) < 0$. However, several bounds on the resolvent and eigenvalue estimates obtained in chapter 5 suggest $\alpha(A) < 0$. The final chapter points to directions in which results presented here might be extended to prove both $\alpha(A) < 0$ and $\alpha(A) = \omega(A)$.

Chapter 2

A Menagerie of Wave Operators

In this chapter, I discuss three operators that are similar to the magnetic damping operator. Two of these operators correspond to Kelvin-Voigt and viscous damping. Like magnetic damping, these two operators are parametrized by a map $a : [0, \pi] \rightarrow \mathbb{R}$. In particular, work on the viscous damping operator by Cox and Zuazua [7] inspires many of the results seen in Chapter 3. Both Kelvin-Voigt and viscous damping operators differ from the magnetic damping operator given in equation (1.2) by the entry in the (2, 2) block. First, however, the undamped wave operator will be reviewed, in which the (2, 2) block is the zero operator. This operator is the limit of Kelvin-Voigt, viscous, and magnetic damping for the constant map $a(x) \equiv \gamma \rightarrow 0$. Finally, at the end of this chapter, I will include a brief discussion of previous work on the magnetic damping operator.

First, a few preliminaries. Each operator is posed on a subspace of $X = H_0^1(0, \pi) \times L^2(0, \pi)$ with energy inner product $\langle \cdot, \cdot \rangle_X$ as defined in equation (1.3). An orthonormal basis for $H_0^1(0, \pi)$ defined by

$$\phi_n(x) = \sqrt{2/\pi} \sin(nx), \quad n = 1, 2, 3, \dots \quad (2.1)$$

is useful in constructing eigenvectors of both Kelvin-Voigt and viscous damping operators.

2.1 Undamped wave operator

A starting point for the study of damped wave operators is the undamped equation

$$\begin{aligned}\frac{\partial^2 u}{\partial t^2}(x, t) - c^2 \frac{\partial^2 u}{\partial x^2}(x, t) &= 0 \\ u(0, t) = u(\pi, t) &= 0\end{aligned}\tag{2.2}$$

whose origin traces back to Euler, d'Alembert, the Bernoullis, and others [23]. This equation describes the transverse displacement u of a string as a function of space x and time t subject to homogeneous Dirichlet boundary conditions. The c^2 term acts as a scaling between time and space, and so, with appropriate scaling on x or t we can take $c = 1$, as I do for the remainder of this thesis. An equivalent formulation of (2.2) may be obtained by the following technique. First, time differentiation is split into two first derivatives by making the identification $v = u_t$. Then the wave equation (2.2) is written as

$$\begin{aligned}\frac{\partial}{\partial t}u &= v \\ \frac{\partial}{\partial t}v &= c^2 \frac{\partial^2}{\partial x^2}u.\end{aligned}$$

Writing this in matrix form gives

$$\frac{\partial}{\partial t} \begin{bmatrix} u \\ v \end{bmatrix} = \begin{bmatrix} 0 & I \\ \Delta & 0 \end{bmatrix} \begin{bmatrix} u \\ v \end{bmatrix}.$$

Then make the identification $V = [u, v]^T$ and

$$A_0 = \begin{bmatrix} 0 & I \\ \Delta & 0 \end{bmatrix},\tag{2.3}$$

where $\text{Dom}(A_0) = H_0^1(0, \pi) \cap H^2(0, \pi) \times H_0^1(0, \pi)$. The operator A_0 has eigenvalues $\lambda_{\pm n} = \pm in$ for $n \in \mathbb{Z}^+$; as such, $\alpha(A_0) = 0$. Finally note that this operator is skew-adjoint on X (i.e., $A = -A^*$) with eigenfunctions $\Phi_{\pm n}(x) = \phi_n[1/n, \pm i]^T$ that form a

complete orthonormal basis for X . Even if (2.2) is generalized to allow $c : [0, \pi] \rightarrow (0, \infty)$ corresponding to variable density and stiffness, this operator remains skew-adjoint under an appropriately modified energy inner product. These results imply that A_0 is conservative: as defined in equation (1.4), $\mathcal{E}(t) = \mathcal{E}(0)$ for all $t > 0$ — there is no choice of c such that energy in the system decays for any initial condition.

Kelvin–Voigt and viscous damping operators have eigenfunctions associated with eigenvalue λ_n with a similar structure for constant damping: $\Psi_n = \phi_n[1, \lambda_n]$, though the spectrum for both operators is different.

2.2 Kelvin–Voigt damping

The Kelvin–Voigt model is a basic description of viscoelasticity used for modeling a solid, like steel, as the infinitesimal limit of a damper and a spring in parallel. In the linearization, a string with a Kelvin–Voigt interior will obey the equation

$$\frac{\partial^2 u}{\partial t^2}(x, t) - \frac{\partial^2 u}{\partial x^2}(x, t) = \frac{\partial}{\partial x} \left(a(x) \frac{\partial^2 u}{\partial x \partial t}(x, t) \right) \quad (2.4)$$

$$u(0, t) = u(\pi, t) = 0,$$

where u measures the longitudinal displacement and a is nonnegative and proportional to the strength of the damper. This is simply a rescaled version of the equation studied by Chen, Liu, and Liu [6, eq. (1.6)] restricted to constant linear density and stiffness, and Dirichlet boundary conditions. In a similar manner to the undamped wave equation, the equation of motion for the Kelvin–Voigt system (2.4) may be converted to a first order system $V_t = A_{KV}V$, where

$$A_{KV} = \begin{bmatrix} 0 & I \\ \Delta & \nabla a \nabla \end{bmatrix}. \quad (2.5)$$

Here for constant a , $\text{Dom}(A_{KV}) = \{[u, v]^T \in H_0^1(0, \pi) \cap H^2(0, \pi) \times H_0^1(0, \pi) \cap H^2(0, \pi)\}$. In contrast to the magnetic damping operator, the $(2, 2)$ block of A_{KV} is unbounded. The spectrum will tend towards a point in the complex plane as $a(x) \equiv \gamma \rightarrow \infty$, and a can be chosen such that $\alpha(A_{KV}) < 0$.

In contrast to the magnetic damping operator, when $a(x) \equiv \gamma$ is constant, an explicit form for the eigenvalues of A_{KV} can be found. Apply A_{KV} to the vector $V_n = [\phi_n, \lambda_n \phi_n]$, then observe that the following relation must hold for λ_n to be an eigenvalue:

$$\phi_n'' - \lambda_n^2 \phi_n + \gamma \lambda_n \phi_n'' = 0.$$

As $\phi_n'' = -n^2 \phi_n$, this reduces to a scalar equation, quadratic in λ_n , with roots:

$$\lambda_n = \frac{-\gamma n^2}{2} \pm n \sqrt{\frac{\gamma^2}{4} n^2 - 1}. \quad (2.6)$$

An example of this spectrum is plotted in figure 2.1. Observe that in the limit $a(x) \equiv \gamma = 0$, the spectrum of A_0 is recovered. One interesting feature of this spectrum is that for finite $\gamma > 0$, there are only a finite number of nonreal eigenvalues. There has also been interest in exotic variable coefficients a that are supported on a strict subset of the domain; see, e.g., work by Liu and Liu [16] and Renardy [19].

The viscous damping operator discussed in the next section has similar properties to the Kelvin–Voigt operator. Namely, eigenvalues and eigenfunctions may be written explicitly when $a(x) \equiv \gamma$. However, the viscous damping literature provides a more apt template for work on the magnetic damping problem.

2.3 Viscous damping

Viscous damping is an effect due to the drag of the surrounding media on transverse motions of a string. Deriving this operator from the Navier–Stokes equations is fre-

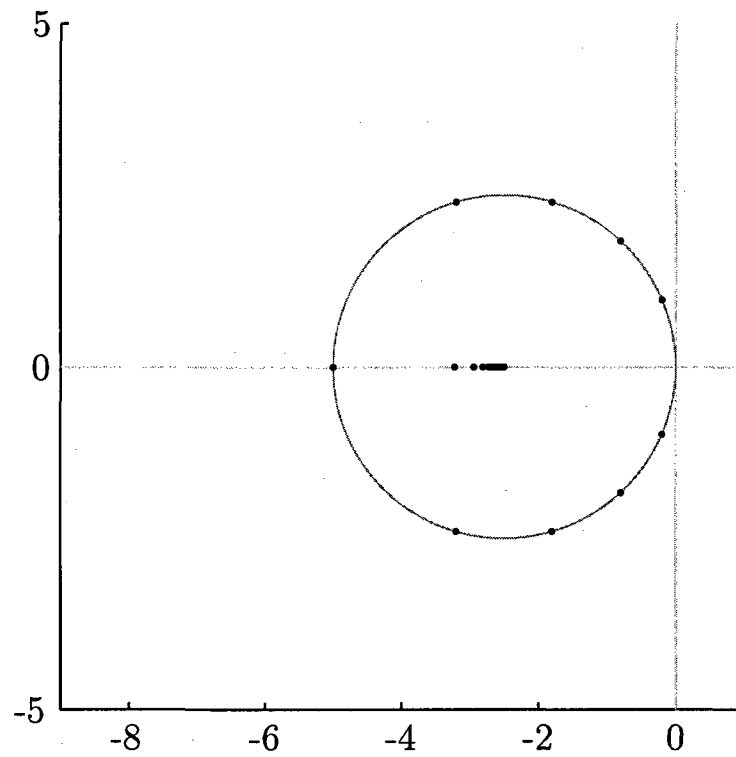


Figure 2.1 : Spectrum of the Kelvin-Voigt damping with constant $a(x) \equiv \gamma = 2/5$. For this choice, A_{KV} has an eigenvalue of multiplicity two at -5 and eight nonreal eigenvalues. The nonreal eigenvalues fall on the circle of radius $2/\gamma$ centered at $-1/\gamma$. Real eigenvalues accumulate at the center of the circle.

quently treated in an ad hoc manner due to the difficulty of coupling these equations to string motion; see, e.g, Batchelor's work [3, pp. 355–358, esp. eq. (5.13.14)]. The derivation assumes a quasi-steady viscous drag acting locally that results in a drag force acting against transverse motion proportional to velocity. Namely,

$$\begin{aligned} \frac{\partial^2 u}{\partial t^2}(x, t) - \frac{\partial^2 u}{\partial x^2}(x, t) &= 2a(x) \frac{\partial u}{\partial t}(x, t), \\ u(0, t) &= u(\pi, t) = 0, \end{aligned} \tag{2.7}$$

where a is nonnegative and proportional to the viscosity of the surrounding fluid and u is the transverse displacement. This approach has some shortcomings as compared to a more elaborate equation of motion given by Lin [15], but (2.7) is studied due to its relative simplicity. Despite this 'simplicity,' this model exhibits rich and complex spectral behavior. Converting equation (2.7) to an operator on X , as with the Kelvin–Voigt problem, results in the evolution problem $V_t = A_{\text{visc}}V$, where

$$A_{\text{visc}} = \begin{bmatrix} 0 & I \\ \Delta & 2a \end{bmatrix}, \tag{2.8}$$

and $\text{Dom}(A_{\text{visc}}) = \{[u, v]^T \in X : u \in H^2(0, \pi) \cap H_0^1(0, \pi), v \in H_0^1(0, \pi)\}$. Observe that if a is bounded, then the (2, 2) block in the operator is bounded, in contrast to the Kelvin–Voigt case, where it is unbounded.

Like the Kelvin–Voigt operator, the spectrum of the viscous damping operator for constant $a(x) \equiv \gamma \geq 0$ can be written explicitly. Applying A_{visc} to $V_n = \phi_n[1, \lambda_n]$ results in a similar scalar equation, quadratic in λ_n , leading to the eigenvalues

$$\lambda_n = -\gamma \pm \sqrt{\gamma^2 - n^2}. \tag{2.9}$$

An example is plotted in figure 2.2. For $\gamma \in [0, 1]$ the spectrum falls on a vertical line in the complex plane with real part $-\gamma$. The first real eigenvalue occurs at $\gamma = 1$, and real eigenvalues result for all $\gamma \geq 1$.

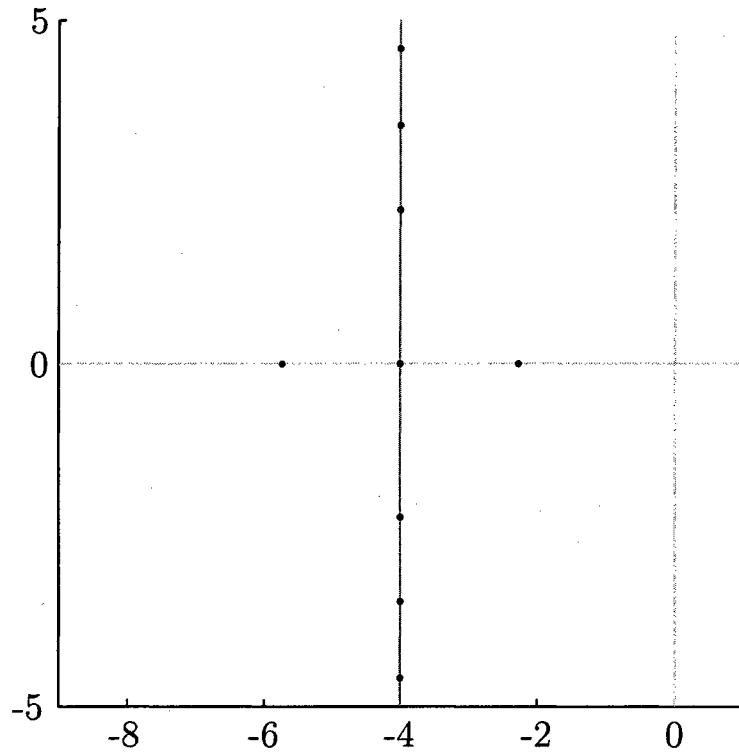


Figure 2.2 : Spectrum of the viscous damping operator with constant $a(x) \equiv \gamma = 2$. For this choice, A_{visc} has an eigenvalue of multiplicity two at -4 and two other real eigenvalues. The nonreal eigenvalues fall on the line $\text{Im}(z) = -\gamma$. As $\gamma \rightarrow \infty$, half of the real eigenvalues tend to $-\infty$ and the other to 0 . The latter eigenvalues are responsible for ‘over damping’ and limit the spectral abscissa.

The affect of a on the spectrum of the viscous damping operator, where $a \in L^\infty$ is nonnegative, was studied by Cox and Zuazua [7], who:

- estimate eigenvalues using a shooting function;
- show that eigenfunctions of the operator form a Riesz basis;
- show the operator has a compact inverse, and hence a discrete spectrum;
- compute the resolvent using a Green's operator;
- obtain asymptotic estimates on eigenvalues using Rouché's theorem; and
- show that the asymptotic decay rate is equivalent to the spectral abscissa using Parseval's equality.

Each of these except the last will have parallels in this thesis.

Once one understands the basic spectral theory for a family of operators, it is natural to investigate design problems: find a such that energy decay is maximized. Cox and Overton considered this problem for generic wave operators on d -dimensional spaces [9]. They conjectured that for viscous damping, $a(x) \equiv \gamma$ for some constant γ was optimal over all $a \in L^\infty$ [9, p. 1355]. Freitas [10] later disputed this conjecture with a numerical counterexample. Using a genetic algorithm he optimized a damping function chosen from a constant plus cosine basis and found a promising example that appeared to move the spectral abscissa further to the left than the optimal constant. In response to Freitas's results, Castro and Cox [5] found a class of damping functions,

$$a(x) = \frac{1}{x + 1/c},$$

that cause the spectral abscissa to become arbitrarily negative as $c \rightarrow \infty$. For the damping function $a(x) = 1/x$, the spectrum is empty and solutions must exhibit extinction in finite time.

A similar damping function, $a(x) = 2/(\pi x)$, inspired by the above, seems to perform well for the magnetic damping problem, as discussed in section 5.4.

2.4 Magnetic damping

Magnetic damping corresponds to an elastic vibrating string in an external magnetic field, as derived in Appendix A. The equation of motion is

$$\frac{\partial^2 u}{\partial t^2} - \frac{\partial^2 u}{\partial x^2} = -a(x) \int_0^\pi a(\xi) \frac{\partial}{\partial t} u(\xi, t) d\xi$$

$$u(0, t) = u(\pi, t) = 0. \quad (2.10)$$

Posing this problem on X results in the operator

$$A = \begin{bmatrix} 0 & I \\ \Delta & -a\langle \cdot, a \rangle \end{bmatrix}, \quad (2.11)$$

where $\text{Dom}(A) = \{[u, v]^T : u, v \in H_0^1(0, \pi), u'' - a\langle v, a \rangle \in L^2(0, \pi)\}$ and $A : \text{Dom}(A) \rightarrow X$. Note in contrast to both Kelvin–Voigt and viscous damping operators, here a is allowed to be both positive and negative.

Magnetic damping has been treated in only two published papers to my knowledge: first by Leibowitz and Ackerberg in 1963 [14] and second by Wolfe in 1998 [24]. Leibowitz and Ackerberg first studied magnetic damping to modify the tonal quality of a piano string, that is, the rate at which each mode decays. To derive the equations of motion, the authors presume that the transverse displacements of the string are small and then apply the effect of a constant magnetic field. For a constant field, where $a(x) \equiv \gamma$, they constructed two proofs — one using Rouché’s theorem, the other based on perturbation theory — bounding the location of eigenvalues λ_n :

$$\lambda_n = \begin{cases} in, & n \text{ even;} \\ in - \frac{4\gamma^2}{n^2} + O(\gamma^4), & n \text{ odd.} \end{cases} \quad (2.12)$$

They also obtained a formula for the eigenvalues of the nonconstant case in terms of a Green's function [14, eq. A6]. No results were derived for general a , although the equations of motion were stated in the appendix [14, eq. A1].

Wolfe approached magnetic damping from a far more rigorous mathematical perspective [24]. Like Leibowitz and Ackerberg, he considered only the constant magnetic field case, but he did address variable string density. He rigorously derived the equations, starting from a full 3D nonlinear elasticity model and then linearizing around a rest state in a manner similar to Antman [2, Ch. 2]. Wolfe constructed proofs of existence and uniqueness using a Galerkin method on the corresponding weak formulation of the partial differential equation. At the end he asks if magnetic damping is strong enough to prevent the formation of shocks in the nonlinear problem; this question has not yet been answered.

A third paper is currently under development by Cox, Embree, Kelm and I on the magnetic damping problem [8]. Many of the results from this paper are described in this thesis, particularly those results appearing in chapters 3 and 4. In those chapters, our results establish that $\sigma(A)$ contains only eigenvalues when $a(x) \leq Cx^p(\pi - x)^p$ for $p > -3/2$ and $C > 0$, and that, for $a \in BV(0, \pi)$, the spectral abscissa matches the decay rate which is zero, $\alpha(A) = \omega(A) = 0$. These results are explained in further detail in the following chapters.

In contrast to Kelvin–Voigt and viscous damping, there is no simple expression for the eigenvalues of the magnetic damping operator for even constant a . In the case that $a(x) \equiv \gamma$, the eigenvalues of A must be written as the roots of the transcendental equation

$$\gamma^2 = \frac{-\lambda^2 \sinh(\lambda\pi)}{(\cosh(\lambda\pi) - 1)^2 - \sinh(\lambda\pi)(\sinh(\lambda\pi) + \lambda\pi)}. \quad (2.13)$$

This result follows from a similar argument from the viscous case. A more general

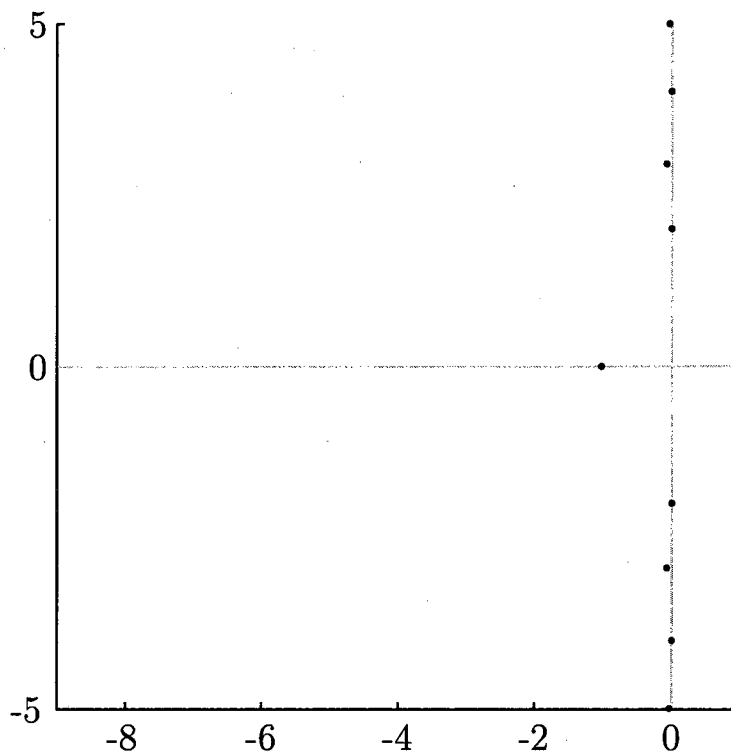


Figure 2.3 : Spectrum of the magnetic damping operator with constant $a(x) \equiv \gamma = 0.8745$. This choice of γ approximates the γ for which the first real eigenvalue of A emerges. For that constant damping, the double eigenvalue is located at approximately -1.0225 . Note that $\pm 2in$ for $n = 1, 2, 3, \dots$ are still eigenvalues. Odd eigenvalues move on the order of $1/n$ to the left of their undamped values, as allowed by Theorem 3.

form is given in Theorem 2 in section 3.3 below. As is expected, when $\gamma = 0$, the resulting equation is simply $\sinh(\lambda\pi) = 0$, which has roots $\lambda = \pm in$.

Chapter 3

Basic Results for Magnetic Damping

In the previous chapter, I discussed the history of magnetic damping and mentioned that many results would follow the approach of Cox and Zuazua [7] for the viscous damping problem. This chapter proves that $\sigma(A)$ contains only eigenvalues of finite multiplicity. The result parallels [7, Thm. 3.1], and is included in [8]. First, an explicit form for the resolvent of A is constructed through the use of a Green's function. The second section will prove that A^{-1} is compact, and thus every point in the spectrum is an eigenvalue. Finally, an equivalence between roots of a shooting function and eigenvalues of A is demonstrated.

This chapter and the succeeding one will make use of the separability of X . When a has singularities diverging slower than $x^{-3/2}$ at both 0 and π , e.g.,

$$|a(x)| \leq Cx^p(\pi - x)^p$$

for some $C > 0$ and $p > -3/2$, an orthonormal basis for $\text{Dom}(A)$ is given by

$$\Phi_{\pm n} = \frac{\phi_n}{\sqrt{2}} \begin{bmatrix} 1/n \\ \pm i \end{bmatrix}, \quad n = 1, 2, 3, \dots, \quad (3.1)$$

where the ϕ_n functions are the orthonormal basis vectors for $H_0^1(0, \pi)$ as defined by equation (2.1). These $\Phi_{\pm n}$ are the eigenfunctions of the undamped wave operator. Additionally, for brevity, the n th Fourier coefficient of a will be noted as

$$a_n = \langle a, \phi_n \rangle.$$

With these definitions, we are prepared to approach this problem.

3.1 Explicit form for the resolvent

Forming the resolvent requires two steps. First $(A - \lambda)^{-1}$ is explicitly constructed in terms of its component block operators and an as yet undetermined Green's operator. Then this Green's operator is constructed from the left and right shooting functions y and w of the associated linear operator \mathcal{L}_λ to be defined in (3.5). Once constructed, this expression for the resolvent is used in section 3.2 to determine that A has a compact inverse. The shooting functions will also provide an alternative means of estimating eigenvalues, as shown in section 3.3.

3.1.1 Inverting $A - \lambda$ via triangular factorization

The resolvent, $(A - \lambda)^{-1}$, is constructed by formally inverting $A - \lambda$ by a triangular factorization. For simplicity, assign

$$A - \lambda = \begin{bmatrix} -\lambda & I \\ \Delta & -a\langle \cdot, a \rangle - \lambda \end{bmatrix} = \begin{bmatrix} B(\lambda) & C \\ D & E(\lambda) \end{bmatrix}. \quad (3.2)$$

Using this form, consider the decomposition

$$A - \lambda = \begin{bmatrix} B(\lambda)^{1/2} & 0 \\ DB(\lambda)^{-1/2} & Q(\lambda)^{1/2} \end{bmatrix} \begin{bmatrix} B(\lambda)^{1/2} & B(\lambda)^{-1/2}C \\ 0 & Q(\lambda)^{1/2} \end{bmatrix} = L(\lambda)U(\lambda),$$

where $Q(\lambda) = E(\lambda) - DB(\lambda)^{-1}C$. Then note the inverses of L and U take the form

$$L(\lambda)^{-1} = \begin{bmatrix} B(\lambda)^{-1/2} & 0 \\ -Q(\lambda)^{-1/2}DB(\lambda)^{-1} & Q(\lambda)^{-1/2} \end{bmatrix},$$

$$U(\lambda)^{-1} = \begin{bmatrix} B(\lambda)^{-1/2} & -B(\lambda)^{-1}CQ(\lambda)^{-1/2} \\ 0 & Q(\lambda)^{-1/2} \end{bmatrix}.$$

Thus the resolvent may be formally written as

$$(A - \lambda)^{-1} = \begin{bmatrix} B(\lambda)^{-1}(I + CQ(\lambda)^{-1}DB(\lambda)^{-1}) & -B(\lambda)^{-1}CQ(\lambda)^{-1} \\ -Q(\lambda)^{-1}DB(\lambda)^{-1} & Q(\lambda)^{-1} \end{bmatrix}. \quad (3.3)$$

At this juncture, note that $B(\lambda) = \lambda I$ is trivially invertible away from $\lambda = 0$; only the term $Q(\lambda) = (1/\lambda)\Delta - a\langle \cdot, a \rangle - \lambda$ poses difficulty. Suppose we can find some $G(\lambda)$ such that $G(\lambda)Q(\lambda) = \lambda$. Then the resolvent may be written in two similar forms:

$$\begin{aligned} (A - \lambda)^{-1} &= \begin{bmatrix} (1/\lambda)(I - G(\lambda)\Delta) & G(\lambda) \\ G(\lambda)\Delta & \lambda G(\lambda) \end{bmatrix} \\ &= \begin{bmatrix} G(\lambda)(\lambda I + a\langle \cdot, a \rangle) & G(\lambda) \\ I + \lambda G(\lambda)(\lambda I + a\langle \cdot, a \rangle) & \lambda G(\lambda) \end{bmatrix}. \end{aligned} \quad (3.4)$$

Alternating between these two forms makes use of the identity $G(\lambda)\Delta = \lambda(\lambda I + \lambda G(\lambda) + G(\lambda)a\langle \cdot, a \rangle)$. A simple calculation shows that the form of the inverse on the right in (3.4) holds for all $\lambda \notin \sigma(A)$.

One way to construct $G(\lambda)$ would be to construct a Green's function $g(x, \xi, \lambda)$ for the operator

$$\mathcal{L}_\lambda = \frac{d^2}{dx^2} - \lambda^2 - \lambda a\langle \cdot, a \rangle, \quad (3.5)$$

since $G(\lambda)\mathcal{L}_\lambda = I$. Then $G(\lambda)$ could be defined through

$$(G(\lambda)v)(\xi) = \int_0^\pi g(x, \xi, \lambda)v(x) dx. \quad (3.6)$$

The next section describes how $g(x, \xi, \lambda)$ is constructed.

3.1.2 Green's function

The Green's function for \mathcal{L}_λ may be constructed from the left and right shooting functions

$$y(x) = \frac{\sinh(\lambda x)}{\lambda} + \frac{\int_0^\pi a(y) \sinh(\lambda y) dy \int_0^x a(y) \sinh(\lambda(x-y)) dy}{\lambda - \lambda \int_0^\pi a(y) \int_0^y a(z) \sinh(\lambda(y-z)) dz dy}, \quad (3.7)$$

$$w(x) = \frac{\sinh(\lambda(\pi-x))}{\lambda} + \frac{\int_0^\pi a(y) \sinh(\lambda y) dy \int_x^\pi a(y) \sinh(\lambda(x-y)) dy}{\lambda - \lambda \int_0^\pi a(y) \int_y^\pi a(z) \sinh(\lambda(y-z)) dz dy}, \quad (3.8)$$

which satisfy the ordinary differential equations $\mathcal{L}_\lambda y = 0$ and $\mathcal{L}_\lambda w = 0$ subject to the initial conditions $y(0) = 0$; $y'(0) = 1$ and $w(\pi) = 0$; $w'(\pi) = -1$. Using these two solutions, the Green's function for \mathcal{L}_λ may be written as

$$g(x, \xi, \lambda) = \begin{cases} \frac{w(\xi, \lambda)y(x, \lambda)}{y(\xi, \lambda)w'(\xi, \lambda) - y'(\xi, \lambda)w(\xi, \lambda)}, & 0 \leq x \leq \xi \leq \pi; \\ \frac{y(\xi, \lambda)w(x, \lambda)}{y(\xi, \lambda)w'(\xi, \lambda) - y'(\xi, \lambda)w(\xi, \lambda)}, & 0 \leq \xi \leq x \leq \pi. \end{cases} \quad (3.9)$$

This formulation satisfies the relation

$$\mathcal{L}_\lambda \int_0^\pi g(x, \xi, \lambda)v(x) dx = v$$

and the boundary conditions, $g(0, \xi, \lambda) = g(\pi, \xi, \lambda) = 0$. A typical example of one such Green's function is shown in figure 3.1. With this definition, $(A - \lambda)^{-1}$ is defined explicitly. The next section will make use of this result to establish that A^{-1} is Hilbert-Schmidt, and hence $\sigma(A)$ contains only eigenvalues.

3.2 Discrete spectra

To show that all points in the spectrum of A are eigenvalues, it is sufficient to show that A has a compact inverse. If A^{-1} is compact, then by the spectral theorem for compact operators, every nonzero point $\lambda \in \sigma(A^{-1})$ is an eigenvalue with an

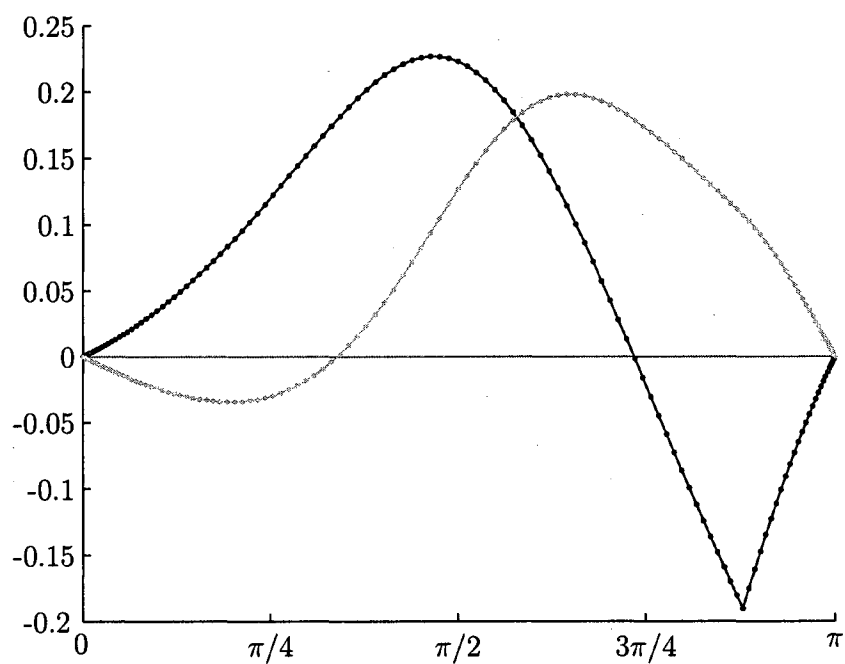


Figure 3.1 : The Green's function $g(x, \xi, \lambda)$ for $\xi \approx 2.75$, $\lambda = -1 + \frac{3}{2}i$, and $a(x) \equiv 1$. Black denotes the real component; gray the imaginary. Dots reflect the Chebyshev grid on which g is discretized, following Appendix B with $N = 128$. The discontinuity in the derivative of $g(x, \xi, \lambda)$ at $x = \xi$ is due to the construction of g .

associated finite dimensional eigenspace. Thus for the eigenpair (λ, V) of A^{-1} , with $\lambda \neq 0$, we have

$$AV = \lambda^{-1}V. \quad (3.10)$$

Before continuing, a restriction must be placed on a to facilitate the analysis of this operator. As in [8], I will only permit a to have singularities at the ends of the domain, controlled in the sense that there exists $C > 0$ such that for all $x \in (0, \pi)$

$$|a(x)| \leq Cx^p(\pi - x)^p, \quad p > -3/2, \quad (3.11)$$

Those a that obey this property will be called *singular*. These singular a have two special properties: their Fourier coefficients do not grow with increasing frequency, and $\langle f, a \rangle$ is bounded for $f \in H_0^1(0, \pi)$. These two statements are not trivially equivalent when $a \notin L^2(0, \pi)$ and so will be established in the two lemmas below.

Lemma 1. *If a obeys the bound (3.11), then $\langle f, a \rangle < \infty$ for all $f \in H_0^1(0, \pi)$.*

Proof. To demonstrate this, observe that for $f \in H_0^1(0, \pi)$, by Hardy's inequality [4, p. 147],

$$\left\| \frac{f(x)}{x(\pi - x)} \right\| \leq C \|f'(x)\|. \quad (3.12)$$

The inner product may be bounded by

$$|\langle f, a \rangle| \leq C \int_0^\pi |f(x)| x^p (\pi - x)^p dx.$$

As $fx^{-1}(\pi - x)^{-1}$ and $x^{p+1}(\pi - x)^{p+1}$ are both in $L^2(0, \pi)$, this integral may be bounded by Cauchy-Schwarz inequality

$$|\langle f, a \rangle| \leq C \left(\int_0^\pi \left| \frac{f(x)}{x(\pi - x)} \right|^2 dx \right)^{1/2} \left(\int_0^\pi x^{p+1} (\pi - x)^{p+1} dx \right)^{1/2}. \quad (3.13)$$

This finite, and so provided a obeys (3.11), the inner product $\langle f, a \rangle$ is bounded for all $f \in H_0^1(0, \pi)$. \square

Lemma 2. *If there exists $C > 0$ such that for all $x \in (0, \pi)$ then $|a(x)| \leq Cx^p(\pi - x)^p$ for $p > -3/2$, then $a_n = O(1)$ as $n \rightarrow \infty$.*

Proof. This is handled as two separate cases. When $p \geq 0$, then

$$|a_n| \leq \int_0^\pi |a(x)| |\sin(nx)| dx \leq \int_0^\pi |a(x)| dx < \infty$$

and hence $|a_n| = O(1)$.

In the other case where $-3/2 < p < 0$, first note that

$$|a_n| \leq \int_0^\pi |\sin(nx)| |a(x)| dx \leq C \int_0^\pi |\sin(nx)| x^p (\pi - x)^p dx.$$

The last integral is symmetric about $\pi/2$ and thus it is sufficient bound the growth of the Fourier coefficient on one half of the domain. On the left half, the $(\pi - x)^p$ term may be bounded above by a constant, giving

$$\int_0^{\pi/2} |\sin(nx)| x^p (\pi - x)^p dx \leq 2(\pi/2)^{-3/2} \int_0^{\pi/2} |\sin(nx)| x^p dx.$$

The integrand on the right above may be decomposed into the product of $\sin(nx)/x$ and x^{p+1} . Since $\sin(nx)/x$ is continuous and bounded above by n for all $x \in (0, \pi/2)$, it is in $L^2(0, \pi)$; the x^{p+1} is also in $L^2(0, \pi)$ since $p + 1 > -1/2$. Applying the Cauchy-Schwarz inequality yields

$$\int_0^{\pi/2} \left| \frac{\sin(nx)}{x} \right| x^{p+1} dx \leq n \left(\int_0^{\pi/2} \left| \frac{\sin(nx)}{nx} \right|^2 dx \right)^{1/2} \left(\int_0^{\pi/2} x^{2(p+1)} dx \right)^{1/2}. \quad (3.14)$$

Now this bound must be shown to be independent of n . To demonstrate this, rescale the $\sin(nx)/(nx)$ integral and split it, giving

$$\begin{aligned} n \int_0^{\pi/2} \left| \frac{\sin(nx)}{nx} \right|^2 dx &= \int_0^{n\pi/2} \left(\frac{\sin(y)}{y} \right)^2 dy \\ &= \int_0^{\pi/2} \left(\frac{\sin(y)}{y} \right)^2 dy + \int_{\pi/2}^{n\pi/2} \left(\frac{\sin(y)}{y} \right)^2 dy. \end{aligned}$$

The integral on the bottom left in the above equation may be bounded by noting $|\sin(y)/y| \leq 1$; the term on the bottom right may be bounded too, since $|\sin(y)/y| \leq 1/y$. This results in

$$\int_0^{n\pi/2} \left(\frac{\sin(y)}{y} \right)^2 dy \leq \frac{\pi}{2} + \frac{2(n-1)}{n\pi} \leq \frac{\pi}{2} + \frac{2}{\pi}.$$

The second integral on the right of (3.14) may be explicitly computed, as $p > -3/2$:

$$\int_0^{\pi/2} x^{2(p+1)} dx = \frac{1}{2p+3} \left(\frac{\pi}{2} \right)^{2p+3}.$$

Collecting all the terms forms the final bound on a_n :

$$|a_n| = \left| \int_0^\pi \sin(nx) a(x) dx \right| \leq \frac{2C}{\sqrt{2p+3}} \left(\frac{\pi}{2} + \frac{2}{\pi} \right)^{1/2} \left(\frac{\pi}{2} \right)^{1/2}.$$

This bound is independent of n and thus $|a_n| = O(1)$. \square

Using these lemmas, the following theorem establishes A^{-1} is Hilbert–Schmidt and thus $\sigma(A)$ contains only eigenvalues.

Theorem 1. *If a obeys the bound (3.11), then A has a discrete spectrum.*

Proof. First, we establish that A^{-1} is compact. Observe that equation (3.4) gives A^{-1} explicitly when $\lambda = 0$. In this case $\mathcal{L}_0 = d^2/dx^2$, so the corresponding Green's function is

$$g(x, \xi, 0) = \begin{cases} \frac{(\pi-\xi)x}{\pi}, & x < \xi; \\ \frac{(\pi-x)\xi}{\pi}, & x > \xi; \end{cases} \quad (3.15)$$

which is the limit of (3.9) as $\lambda \rightarrow 0$. Observe that

$$A^{-1}\Phi_{\pm n} = \frac{1}{\sqrt{2}} \begin{bmatrix} \frac{1}{n}G(0)a\langle \phi_n, a \rangle \pm iG(0)\phi_n \\ \frac{1}{n}\phi_n \end{bmatrix}. \quad (3.16)$$

Thus splitting the above term into the sum of three vectors and applying the triangle inequality yields

$$\sqrt{2}\|A^{-1}\Phi_{\pm n}\|_{L(X)} \leq \frac{1}{n}|a_n| \|(G(0)a)'\| + \|(G(0)\phi_n)'\| + \frac{1}{n}\|\phi_n\|. \quad (3.17)$$

Looking at the final term on the right of (3.17), as ϕ_n are orthonormal on $L^2(0, \pi)$, we have $\|\phi_n\| = 1$. For the second term on the right, note that

$$G(0)\phi_n = -\frac{1}{n^2}\phi_n. \quad (3.18)$$

Thus $\|(G(0)\phi_n)'\| = 1/n$.

The first term on the right of (3.17) is the most cumbersome. By lemma 2, $a_n = O(1)$, so this term does not grow with n . Finally, $\|(G(0)a)'\|$ needs to be bounded. Regardless of which p is chosen for the bound in (3.11), an upper bound can always be constructed with $p < 0$. Taking the derivative of

$$(G(0)a)(\xi) = \frac{\pi - \xi}{\pi} \int_0^\xi xa(x) dx + \frac{\xi}{\pi} \int_\xi^\pi (\pi - x)a(x) dx,$$

the terms involving the derivatives of $\int_0^\xi xa(x) dx$ and $\int_\xi^\pi (\pi - x)a(x) dx$ cancel, leaving

$$\begin{aligned} |(G(0)a)'(\xi)| &= \left| \frac{-1}{\pi} \int_0^\xi xa(x) dx + \frac{1}{\pi} \int_\xi^\pi (\pi - x)a(x) dx \right| \\ &\leq \frac{C}{\pi} \left(\int_0^\xi x^{p+1}(\pi - x)^p dx + \int_\xi^\pi x^p(\pi - x)^{p+1} dx \right) \\ &\leq C\pi^{2p+1} (B_{\xi/\pi}(p+2, p+1) + B_{(\pi-\xi)/\pi}(p+2, p+1)) \end{aligned}$$

where B is the incomplete Euler beta function. This is bounded and square integrable on $(0, \pi)$, thus $\|(G(0)a)'\| < \infty$. So the first term on the right in (3.17) is $O(1/n)$. Since every term on the right of (3.17) is $O(1/n)$, we conclude $\|A^{-1}\Phi_{\pm n}\|_X = O(1/n)$.

Thus A^{-1} is Hilbert-Schmidt as,

$$\|A^{-1}\|_{HS}^2 = \sum_n \|A^{-1}\Phi_{\pm n}\|_X^2 < \infty,$$

and so also compact. Therefore, by the Fredholm Alternative, $\sigma(A)$ contains only point spectrum; see, e.g. [18, Thm. VI.14]. \square

Additionally, the term $\|(G(0)a)'\|$ plays a role in a bound proved in section 5.2. There, an upper bound on the resolvent is constructed whose poles, and hence possible locations for eigenvalues, hinge on $\|(G(\lambda)a)'\|$.

The next section proves that when $y(\pi, \lambda) = 0$, this λ is an eigenvalue of A .

3.3 Shooting function

The left and right shooting functions provide a technique to compute the spectrum of A . The following theorem establishes that the roots of shooting functions are indeed equivalent to eigenvalues.

Theorem 2. *For the left shooting function y given in equation (3.7), $y(\pi, \lambda) = 0$ if and only if $\lambda \in \sigma(A)$.*

Proof. If $y(\pi, \lambda) = 0$, then $V = y[1, \lambda]^T \in X$. Applying $A - \lambda$ to V ,

$$(A - \lambda)V = \begin{bmatrix} 0 \\ y_2'' - \lambda a\langle y, a \rangle - \lambda^2 y \end{bmatrix}.$$

However, as y satisfies $y'' - \lambda^2 y - \lambda a\langle y, a \rangle = 0$ by construction, then $(A - \lambda)V = 0$ and V is an eigenvector associated with eigenvalue λ .

If $\lambda \in \sigma(A)$, then there must exist an eigenvector $V = [u, v] \in X$. Then

$$(A - \lambda)V = \begin{bmatrix} -\lambda u + v \\ u'' - \lambda a\langle v, a \rangle - \lambda^2 v \end{bmatrix} = \begin{bmatrix} 0 \\ 0 \end{bmatrix}.$$

The first entry gives $v = \lambda u$, while the second then requires

$$v'' - \lambda^2 v - \lambda a\langle v, a \rangle = 0.$$

This integro-differential equation has the two linearly independent solutions $y(x, \lambda)$ and $w(x, \lambda)$ given in equations (3.7) and (3.8). These satisfy the left and right boundary conditions respectively. In order for a linear combination of these to satisfy both boundary conditions, we must have $y(\pi, \lambda) = 0$ and $w(0, \lambda) = 0$, as required. \square

In this section I have shown that $\sigma(A)$ contains only eigenvalues. These eigenvalues may be estimated by roots in λ of the shooting function $y(\pi, \lambda)$. With equal validity, $w(0, \lambda) = 0$ implies that λ is an eigenvalue of A . The next section will develop bounds on the spectrum of A , but also cite an important result from [8] that for bounded variation fields, energy does not asymptotically decay for all initial conditions.

Chapter 4

Bounded Variation Fields

If maximizing energy decay is the design objective, then bounded variation fields are inadequate, as shown in [8]. In this chapter I will cite the critical result from [8] that for bounded variation fields a , $\lambda_{\pm n}$ approaches $\pm in$ with an error of $O(1/n)$ as $n \rightarrow \infty$. This proof will be outlined in Theorem 3 below. Then Theorem 4 shows that Theorem 3 is sufficient give $\alpha(A) = \omega(A)$. Section 4.2 will present several bounds on $\sigma(A)$ in terms of $\|a\|$. Then section 4.3 establishes a new bound on the resolvent of A in terms of the Fourier coefficients a_n . Finally, I will conclude with two examples of a : a single sinusoid in section 4.4 and multiple sinusoids in section 4.5, both of which come from [8]. These examples demonstrate the bounds derived in the preceding sections and point to the need for singular damping functions, i.e., those divergent at some point $x \in [0, \pi]$, as analyzed in chapter 5.

4.1 Spectral abscissa for bounded variation a

The following result follows from [8, prop. 4.2].

Theorem 3. *Suppose $a \in BV(0, \pi)$ and let $AV_{\pm n} = \lambda_{\pm n}V_{\pm n}$ for $n = \mathbb{Z}^+$. One can order eigenvalues such that if $a_n = 0$, then $\lambda_n = in$ and $V_n = \Phi_{\pm n}$ and if $a_n \neq 0$, then*

$$\lambda_{\pm n} = \pm in + O(1/n) \quad \text{and} \quad V_{\pm n} = \Phi_{\pm n} + O(1/n).$$

The set of vectors $\{V_n : n = \pm 1, \pm 2, \pm 3, \dots\}$ is a Riesz basis for X .

The proof of this results follows a similar technique to that of Cox and Zuazua [7, Thm. 5.1 & 5.3], sketched below. First a bound on the eigenvalues establishes that they reside in the slab $\{\lambda : -\frac{1}{2}\|a\| \leq \operatorname{Re}(\lambda) \leq 0\}$ (as shown in Theorem 5 below). Then a series of telescoping balls are constructed, centered at $\pm in$ for $n = 1, 2, 3, \dots$, with decreasing radius proportional to $1/n$. A bound establishes that $|y(\pi, \lambda) - \lambda^{-1} \sinh(\lambda\pi)| \leq |\lambda^{-1} \sinh(\lambda\pi)|$ on the boundary of these disks for sufficiently large n . Then Rouché's theorem implies that $\lambda^{-1} \sinh(\lambda\pi)$ and $y(\pi, \lambda)$ have the same number of zeros on the interior of these disks. Thus as $n \rightarrow \infty$, each disk contains one root. As these disks are of decreasing radius, the roots approach $\pm in + O(1/n)$.

Since $-a\langle \cdot, a \rangle$ is bounded, then A a bounded perturbation away from A_0 , a skew-adjoint operator. Thus the eigenvectors of A , V_n , form a Reisz basis, due to a theorem of Gohberg and Krein [11, Ch. 5, Thm. 10.1]. The spectral abscissa will then determine the asymptotic decay rate, following Cox and Zuazua [7, Thm. 6.4].

Theorem 4. *If $a \in BV(0, \pi)$ then $\alpha(A) = \omega(A)$.*

Proof. From Theorem 3, $\{V_{n,j} : n = \pm 1, \pm 2, \pm 3, \dots; j = 0, \dots, m_n - 1\}$ forms a Reisz basis for X , where m_n is bounded above and denotes the dimension of subspace associated with the n th eigenvalue. Hence, eigenvectors $V_{n,1}, V_{n,2}, \dots, V_{n,m_n}$ share the same eigenvalue λ_n . Thus any initial condition V may be written as a linear combination of elements $V_{n,j}$. Expanding both V and \mathcal{E} in this basis yields

$$V = \sum_{n \in \mathbb{Z}} \sum_{n \neq 0} \sum_{j=0}^{m_n-1} \alpha_{n,j} V_{n,j}$$

$$\mathcal{E}(t) \leq \mathcal{E}(0) \sum_{n \in \mathbb{Z}} \sum_{n \neq 0} \sum_{j=0}^{m_n-1} |\alpha_{n,j}|^2 |t^{2j}| |e^{2t\lambda_n}| \|V_{n,j}\|^2.$$

As demonstrated in [8, Prop. 4.2], there are most some finite number, say N , eigenvalues of algebraic multiplicity greater than one. Thus there exists a C such that

$$\mathcal{E}(t) \leq C\mathcal{E}(0)(1 + t^N)e^{2\alpha(A)t}.$$

This establishes $\omega(A) \leq \alpha(A)$. The other direction of the inequality also holds as mentioned in Chapter 1, and so

$$\omega(A) = \alpha(A).$$

□

Together, Theorems 3 and 4 imply $\omega(A) = 0$. Thus given any decay rate $\mu < 0$, there exists an initial condition such that energy decays at a slower rate than μ . The lack of energy decay for bounded variation fields motivates the study of singular fields in the next chapter. In the following sections, however, several bounds will be constructed illustrating where $\sigma(A)$ must lie for $a \in L^2(0, \pi)$.

4.2 Bounds on the spectrum

The proof of Theorem 3 required a rough bound on the location of $\sigma(A)$. These bounds are constructed by a clever use of inner product identities and bounds, as shown in the following theorem. Here I follow [8, Thm. 2.1(iii) and (iv)].

Theorem 5. *Suppose $\lambda \in \sigma(A)$ and $a \in L^2(0, \pi)$. Then the following bounds hold.*

- (i) *If $\text{Im}(\lambda) \neq 0$ then $\text{Re}(\lambda) \geq -\frac{1}{2}\|a\|^2$.*
- (ii) *If $\text{Im}(\lambda) = 0$ then $\text{Re}(\lambda) \geq -\|a\|^2$.*
- (iii) *$|\lambda| \geq 1$.*

Proof. Recall y , defined equation (3.7), solves the ordinary differential equation $\mathcal{L}_\lambda y$, given by (3.5), obeying boundary conditions on the left. Thus $\mathcal{L}_\lambda y = 0$ by construction. Taking the inner product of $\mathcal{L}_\lambda y$ with y gives

$$\begin{aligned} 0 &= \langle \mathcal{L}_\lambda y, y \rangle = \langle y'', y \rangle - \lambda^2 \langle y, y \rangle - \lambda \langle y, a \rangle \langle a, y \rangle \\ &= -\|y'\|^2 - \lambda^2 \|y\|^2 - \lambda |\langle y, a \rangle|^2; \end{aligned}$$

here the second step uses integration by parts. Although this appears to give a quadratic that explicitly determines λ , it does not, as y depends on λ . To obtain a bound independent of y , note that the roots of this quadratic are given by

$$\lambda = \frac{-|\langle y, a \rangle|^2 \pm \sqrt{|\langle y, a \rangle|^4 - 4\|y'\|^2\|y\|^2}}{2\|y\|^2}. \quad (4.1)$$

Eigenvalues λ are real provided $|\langle y, a \rangle|^2 \geq 2\|y'\|\|y\|$. Assuming so, constructing a lower bound on λ by setting the second term under the root to zero gives

$$\operatorname{Re}(\lambda) \geq -\|a\|^2. \quad (4.2)$$

This establishes part (ii).

Note that when λ is not real, the real and imaginary components in (4.1) may be read off. As $y \in H_0^1(0, \pi)$, Poincaré's (or Wirtinger's) inequality provides $\|y\| \leq \|y'\|$. Using this bound, the real and imaginary components of λ may be bounded below by

$$\begin{aligned} \operatorname{Re}(\lambda) &\geq -\frac{1}{2}\|a\|^2 \\ (\operatorname{Im}(\lambda))^2 &\geq 1 - \frac{1}{4}\|a\|^4. \end{aligned} \quad (4.3)$$

This establishes part (i).

Part (iii) states that λ stays outside of the unit disk, excepting the real line. To show this, simply note when $\lambda \notin \mathbb{R}$, then

$$|\lambda|^2 = (\operatorname{Re}(\lambda))^2 + (\operatorname{Im}(\lambda))^2 \geq 1 \quad (4.4)$$

using the upper bounds given in (4.3). \square

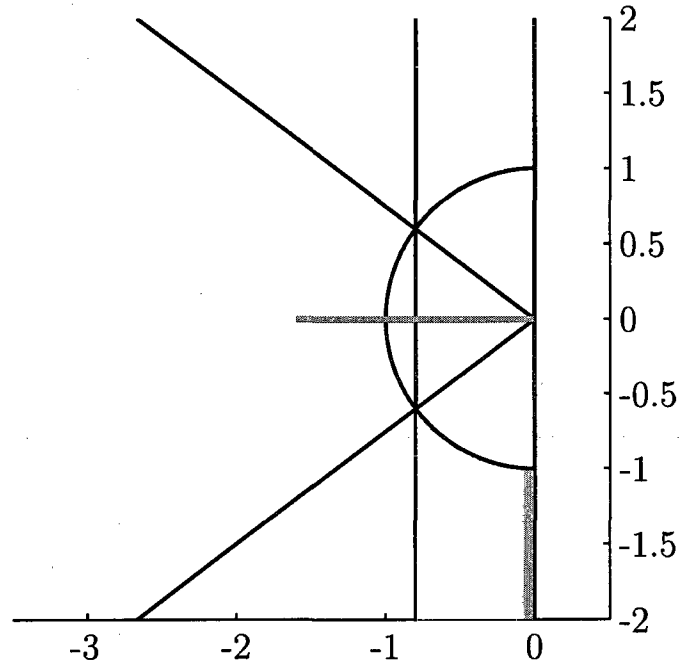


Figure 4.1 : Bounds provided by Theorem 5. The bounds are indicated by black lines. Eigenvalues of A then reside inside the gray regions. Here, $\|a\|^2 = 1.6$. As the norm of a increases, the vertical line moves increasingly to the left and the two diagonal lines collapse onto the real line, at which point they no longer restrict the spectrum on \mathbb{C} .

Another bound established in [8] is on the argument of λ for $\|a\| < 2$. Defining $\text{Re}(\lambda) = |\lambda| \cos \theta$ and $\text{Im}(\lambda) = |\lambda| \sin \theta$, then

$$\frac{\cos^2 \theta}{\sin^2 \theta} \leq \frac{\|a\|^4}{4 - \|a\|^4}.$$

Since these are the components of a right triangle, observe $\cos^2 \theta \leq \|a\|^4/4$ implies θ is within $\arcsin(\|a\|^2/2)$ of $\pi/2$ or $3\pi/2$. As illustrated in figure 4.1, this angle intersects the vertical line (Theorem 5 (i)) and disk (Theorem 5 (iii)) bounds.

An alternative to explicit bounds on the eigenvalues of A is to bound the resolvent of A . The following section establishes a new lower bound providing, a suggestion of where $\sigma(A)$ must reside when a_n is small.

4.3 Resolvent bound in terms of Fourier coefficients

The following is a new result I have established on the norm of the resolvent of A . Assuming the resolvent exists, then a lower bound may be obtained from $(A - \lambda)\Psi$ for some vector Ψ . Observe,

$$\|(A - \lambda)^{-1}\|_{L(X)} \geq \frac{\|(A - \lambda)^{-1}\Psi\|_X}{\|\Psi\|_X} \quad \forall \Psi \in X.$$

Setting $\Psi = (A - \lambda)\Phi$ where $\Phi \in \text{Dom}(A - \lambda)$ and noting the cancellations gives the lower bound on the resolvent of A

$$\frac{\|\Phi\|_X}{\|(A - \lambda)\Phi\|_X} \leq \|(A - \lambda)^{-1}\|_{L(X)} \quad \forall \Phi \in \text{Dom}(A - \lambda). \quad (4.5)$$

Define $\Psi_n = \phi_n[1, \lambda]$ and note that

$$(A - \lambda)\Psi_n = \begin{bmatrix} 0 \\ -n^2\phi_n - \lambda^2\phi_n - \lambda a_n \end{bmatrix}. \quad (4.6)$$

Taking the X -norm of $(A - \lambda)\Psi_n$ and expanding in the orthonormal basis $\Phi_{\pm m}$ yields

$$\|(A - \lambda)\Psi_n\|_X^2 = \sum_{\substack{\pm m \\ m \in \mathbb{Z}^+}} |-n^2\delta_{nm} - \lambda^2\delta_{nm} - \lambda a_n a_m|^2 \quad (4.7)$$

where δ_{mn} denotes the Kronecker delta function. Adding the term $|\lambda a_n^2|^2$ term to the right allows the sum to be decomposed into the $m = n$ term and a term proportional to $\|a\|^2$; thus a lower bound may be written as

$$\|(A - \lambda)\Psi_{\pm n}\|_X^2 \leq |n^2 + \lambda^2 + \lambda a_n^2|^2 + |\lambda|^2 |a_n|^2 \|a\|^2. \quad (4.8)$$

This result leads to Theorem 6.

Theorem 6. *Let $\lambda \in \mathbb{C}$. Provided $a \in L^2(0, \pi)$, then*

$$\frac{n^2 + |\lambda|^2}{|n^2 + \lambda^2 + \lambda a_n^2|^2 + |\lambda|^2 |a_n|^2 \|a\|^2} \leq \|(A - \lambda)^{-1}\|_{L(X)}^2 \quad (4.9)$$

holds for all n .

Note that when $a_n = 0$, taking $\lambda \rightarrow \pm in$ results in an arbitrarily large lower bound on the resolvent, indicating the presence of an eigenvalue. This replicates the result of Theorem 3, which states that when $a_n = 0$, $\pm in$ is an eigenvalue.

Theorem 7 in the next chapter suggests that $\lambda = -\frac{1}{2}a_n^2 \pm in$ are approximate eigenvalues when a_n is small. With this choice of λ , $|n^2 + \lambda^2 + \lambda a_n^2| = 0$. Thus

$$\frac{8n^2 + |a_n|^4}{|a_n|^2(4n^2 + |a_n|^4)\|a\|} \leq \|(A \mp in + \frac{1}{2}|a_n|^2)^{-1}\|_{L(X)}^2. \quad (4.10)$$

This shows that in the limit of small a_n , the resolvent grows as a_n^{-2} here.

The next two sections will detail exact methods for computing eigenvalues when a_n is nonzero for only a finite number of terms.

4.4 A sinusoidal damping field

In the case where $a(x) = \gamma\phi_m(x)$, an analytic expression for the eigenvalues of A can be obtained following [8]. This is made easy since a is an eigenfunction of $\phi'' - m^2\phi = 0$ on $(0, \pi)$. To determine the eigenvalues of A , apply the operator to $\Phi_{\pm n}$, where $\Phi_{\pm n}$ are the eigenfunctions of the undamped operator A_0 as defined by equation (3.1). Then

$$(A \mp in)\Phi_{\pm n} = \frac{1}{\sqrt{2}} \begin{bmatrix} 0 \\ \mp i\phi_n \pm i\phi_n - n\phi_n \mp i\gamma^2\phi_m\langle\phi_m, \phi_n\rangle + n\phi_n \end{bmatrix} = 0.$$

When $n \neq m$, $(A \mp in)\Phi_{\pm n} = 0$. Thus $\pm in$, $n \neq m$, are eigenvalues; this is expected from Theorem 3. For the $n = m$ case, apply A to $\Psi_{\pm m} = \phi_m[1, \pm\lambda]$ to see

$$(A - \lambda)\Psi_{\pm m} = \begin{bmatrix} 0 \\ (m^2 - \lambda\gamma^2 - \lambda^2)\phi_m \end{bmatrix}.$$

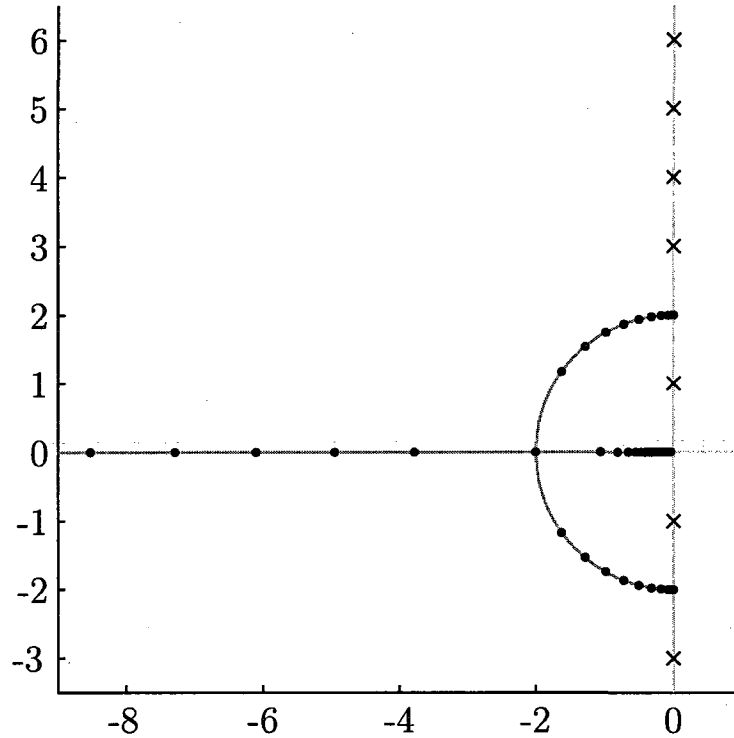


Figure 4.2 : Eigenvalues of A when $a(x) = \gamma\phi_2(x)$. Here eigenvalues of A are marked in black dots as γ ranges from 0 to 10 in steps of $\frac{1}{2}$. These eigenvalues fall on the gray path starting from the imaginary axis, moving towards -2 , after which one goes to 0 and the other to $-\infty$ as $\gamma \rightarrow \infty$. Unperturbed eigenvalues are marked by an \times .

Then $\Psi_{\pm m}$ is an eigenvector provided $m^2 - \lambda\gamma^2 - \lambda = 0$. So the spectrum of A may be written as

$$\sigma(A) = \{\pm in : n \neq m, n = 1, 2, 3, \dots\} \cup \left\{ \frac{-\gamma^2 \pm \sqrt{\gamma^4 - 4m^2}}{2} \right\}. \quad (4.11)$$

Several features are easily noted. For $\gamma < \sqrt{2m}$, all eigenvalues are complex; a real eigenvalue with multiplicity two occurs when $\gamma = \sqrt{2m}$ at $\lambda = -2m$; for $\gamma > \sqrt{2m}$, there are two real eigenvalues: one in $(-\infty, -2m)$; the other in $(-2m, 0)$.

The construction of $\Psi_{\pm m}$ suggests a similar technique when a is composed of a finite number of sinusoids. This is explored in the following section.

4.5 Finite bandwidth a

When $a(x) = \sum_{n \in \mathcal{I}} \gamma_n \sin(nx)$ for some *finite* set of indices $\mathcal{I} \subseteq \{1, 2, 3, \dots\}$, the dimension of the problem can be reduced. As ϕ_n functions are orthogonal, $\Phi_{\pm n}$ is still an eigenvector of A with eigenvalue $\pm in$ provided $n \notin \mathcal{I}$. The remaining eigenvalues can be found via a finite dimensional quadratic eigenvalue problem [8]. Assume the eigenvectors have the form

$$V = \left(\sum_{n \in \mathcal{I}} \alpha_n \phi_n \right) [1, \lambda]^T.$$

As the upper entry in $A - \lambda$ applied to V is zero, so the condition for V to be an eigenvector lies solely with the lower entry,

$$[(A - \lambda)V]_2 = \sum_{n \in \mathcal{I}} \alpha_n n^2 \phi_n - \lambda \sum_{n \in \mathcal{I}} \gamma_n \phi_n \sum_{m \in \mathcal{I}} \alpha_m \gamma_m - \lambda^2 \sum_{n \in \mathcal{I}} \alpha_n \phi_n.$$

This condition on γ_n for λ to be an eigenvalue can be rewritten in terms of one matrix and two vectors. If n_j denotes the j th entry in \mathcal{I} , then these matrices are:

$$[D]_{jk} = \begin{cases} n_j^2, & j = k; \\ 0, & j \neq k, \end{cases}$$

$$[g]_j = \gamma_j,$$

$$[a]_j = \alpha_j.$$

Thus the $\lambda \in \sigma(A)$ associated with damped eigenvectors satisfy a finite-dimensional quadratic eigenvalue problem,

$$\mathcal{Q}(\lambda)\mathbf{a} = (D - \lambda g g^T - \lambda^2 I) \mathbf{a} = 0. \quad (4.12)$$

Of course, the undamped eigenvalues remain at $\lambda_{\pm n} = \pm in$ for all $n \notin \mathcal{I}$.

As this chapter has demonstrated, bounded variation fields, despite their many interesting features seen in the preceding two sections, are ineffective at producing

energy decay. The next chapter will explore fields that diverge at either 0 or π or both. Several results will suggest that $\alpha(A) < 0$ for certain singular fields.

Chapter 5

Singular Damping Fields

As the preceding chapter demonstrated, if $a \in BV(0, \pi)$, then the asymptotic rate of decay, $\omega(A)$, is zero. This lack of energy decay in the bounded variation case prompts the study of singular fields, which are those a such that for some $C > 0$ and $p > -3/2$,

$$|a(x)| \leq Cx^p(\pi - x)^p$$

for all $x \in (0, \pi)$. As described in the two lemmas in section 3.2, this choice of a ensures the Fourier coefficients of a do not grow with increasing frequency and that the inner product $\langle v, a \rangle$ is bounded for all $v \in H_0^1(0, \pi)$. In this chapter I present several novel results. The first section gives an estimate of the rate at which damping functions move eigenvalues away from the imaginary axis. Sections 5.2 and 5.3 give an upper and a lower bound on the norm of the resolvent. These may be used to locate eigenvalues of A and determine asymptotic behavior. The last section presents some numerical experiments to find a damping function that minimizes the spectral abscissa of low frequency eigenvalues.

5.1 Rate of leaving the axis

Here we use the implicit function theorem to obtain the derivative of λ with respect to the strength of the field a .

Theorem 7. *Let a denote a function that satisfies (3.11), and, in a neighborhood $[0, \epsilon)$ for some $\epsilon > 0$, let $\Lambda_n(\gamma)$ denote an eigenvalue of A with damping function*

$a_\gamma(x) \equiv \sqrt{\gamma}a(x)$, with $\Lambda_n(0) = in$ for all $n \in \mathbb{Z} \setminus \{0\}$. Then $\Lambda'_n(0) = -\frac{1}{2}a_{|n|}^2$.

Proof. Define $S(\lambda; a)$ by

$$\begin{aligned} S(\lambda; a) &= \sinh(\lambda\pi) + \int_0^\pi \sinh(\lambda x)a(x) dx \int_0^\pi \sinh(\lambda(\pi - y))a(y) dy \\ &\quad - \sinh(\lambda\pi) \int_0^\pi a(x) \int_0^x \sinh(\lambda(x - y))a(y) dy dx. \end{aligned}$$

Note that $S(\lambda; a)$ is a scaled version of $y(\pi, \lambda)$; as such, roots of $S(\lambda; a)$ correspond to eigenvalues of A . For notational brevity, the following shorthand is introduced for the three components of $S(\lambda; a)$:

$$\begin{aligned} X(\lambda) &= \int_0^\pi \sinh(\lambda x)a(x) dx, \\ Y(\lambda) &= \int_0^\pi \sinh(\lambda(\pi - y))a(y) dy, \\ Z(\lambda) &= \int_0^\pi a(x) \int_0^x \sinh(\lambda(x - y))a(y) dy dx. \end{aligned}$$

Consider the two-variable parametrization $R(\lambda, \gamma) := S(\lambda, \sqrt{\gamma}a)$, so

$$R(\lambda, \gamma) = \sinh(\lambda\pi) + \gamma X(\lambda)Y(\lambda) - \gamma \sinh(\lambda\pi)Z(\lambda). \quad (5.1)$$

First note that $R(in, 0) = 0$ for $n \in \mathbb{Z}$ and $R \in C^1$ (see Rudin [20, Thm. 9.21]).

Denote the partial derivative with respect to the j th component by \mathbf{D}_j . Then provided $\mathbf{D}_1 R$ is nonzero, the implicit function theorem [20, Thm. 9.28] gives a function $\Lambda_n(\gamma)$ defined on $[0, \epsilon)$ where $\epsilon > 0$ such that $R(\Lambda_n(\gamma), \gamma) = 0$ and

$$\Lambda'_n(0) = -\frac{\mathbf{D}_2 R(\lambda, \gamma)|_{\lambda=in, \gamma=0}}{\mathbf{D}_1 R(\lambda, \gamma)|_{\lambda=in, \gamma=0}}.$$

Observe

$$\begin{aligned} \mathbf{D}_1 R(\lambda, \gamma) &= \pi \cosh(\lambda\pi) + \gamma(X'(\lambda)Y(\lambda) + X(\lambda)Y'(\lambda)) \\ &\quad - \gamma\pi \cosh(\lambda\pi)Z(\lambda) - \gamma \sinh(\lambda\pi)Z'(\lambda) \end{aligned}$$

$$\mathbf{D}_2 R(\lambda, \gamma) = X(\lambda)Y(\lambda) - \sinh(\lambda\pi)Z(\lambda).$$

Thus we may conclude that

$$\begin{aligned}\Lambda'_n(0) &= -\frac{X(0)Y(0)}{\pi \cosh(in\pi)} \\ &= -\frac{\int_0^\pi i \sin(nx)a(x) dx (-1)^{n+1} \int_0^\pi i \sin(ny)a(y) dy}{\pi(-1)^n} \\ &= -\frac{1}{\pi} \left(\int_0^\pi \sin(nx)a(x) dx \right)^2 = -\frac{1}{2}a_{|n|}^2.\end{aligned}$$

□

This result matches what one would expect from Theorem 3, which shows $\alpha(A) = 0$ for $a \in BV(0, \pi)$. A result from [17, Cor. 1.4.43] shows that if $a \in BV(0, \pi)$, then $a_n = O(1/n)$, so Theorem 7 predicts $\Lambda'_n(0) \rightarrow 0$ as $n \rightarrow \pm\infty$, matching Theorem 3. Also, the first order approximation of an eigenvalue of A , $\lambda = in + \Lambda'_n(0)$ is special. This choice of λ maximizes the bound given by equation (4.9). However, this bound on the resolvent holds only for bounded variation functions. The following section will detail the particular singular case of $a(x) = \gamma/x$.

5.1.1 Example when $a(x) = \gamma/x$

The study of $a(x) = \gamma/x$ is motivated by its resemblance a function that moves the spectral abscissa uniformly for the viscous damping problem [5]. The Fourier coefficients of this function may be written as:

$$\begin{aligned}\langle a, \phi_n \rangle &= \gamma\sqrt{2/\pi} \int_0^\pi \sin(nx)/x dx = \gamma\sqrt{2/\pi} \int_0^{n\pi} \sin(x)/x dx \\ &= \gamma\sqrt{2/\pi} \text{Si}(n\pi),\end{aligned}\tag{5.2}$$

where Si is the sine integral as defined by Abramowitz and Stegun [1, p. 232]. By taking a Taylor expansion, the values of Si($n\pi$) can be approximated for large n :

$$\text{Si}(\pm n\pi) = \pm\pi/2 \mp (-1)^n/(n\pi) + O(1/n^3).\tag{5.3}$$

Table 5.1 : Comparison of $\Lambda'_n(0)$ as computed by Theorem 7 and a numerical estimate. Here $a(x) = 2/(\pi x)$. Numerical estimates of the derivative are computed by first order approximation: $\tilde{\Lambda}'_n(0) = (\Lambda_n(\epsilon) - \Lambda_n(0))/\epsilon$ for $\epsilon \approx 1.5 \times 10^{-8}$. (This choice of ϵ is the square root of machine precision.) Approximate eigenvalues $\Lambda_n(\epsilon)$ are computed by a spectral discretization of A on a Chebyshev grid size $N = 1024$, as described in Appendix B. Error is the difference between $\Lambda'_n(0)$ and $\tilde{\Lambda}'_n(0)$ divided by $\Lambda'_n(0)$.

| n | $\Lambda'_n(0)$ | $\tilde{\Lambda}'_n(0)$ | Error |
|-----|-----------------|-------------------------|---------|
| 1 | -0.44244787 | -0.44243694 | 0.00693 |
| 2 | -0.25945010 | -0.25943227 | 0.00030 |
| 3 | -0.36183797 | -0.36183510 | 0.00114 |
| 4 | -0.28723568 | -0.28724784 | 0.00009 |
| 5 | -0.34442273 | -0.34440233 | 0.00055 |

Using this approximation, the rate of eigenvalues leaving the imaginary axis may be expressed as

$$\Lambda'_n(0) = -\gamma^2 \frac{1}{\pi} \text{Si}^2(n\pi) = -\gamma^2 \frac{\pi}{4} + O(1/|n|)$$

as $n \rightarrow \infty$. Thus as $n \rightarrow \pm\infty$, each eigenvalue appears to leave the imaginary axis at the same rate. Numerical experiments confirm this result, as seen in Table 5.1

5.2 Resolvent upper bound

Here I will obtain an upper bound on the resolvent by using the undamped operator A_0 , (i.e. A with $a(x) \equiv 0$). To do so note the action of $(A - \lambda)^{-1}$ on $A_0 - \lambda$ when $\lambda \notin \sigma(A_0) \cup \sigma(A)$ we formally have

$$(A - \lambda)^{-1} = (A - \lambda)^{-1}(A_0 - \lambda)(A_0 - \lambda)^{-1},$$

which suggests the expansion

$$(A - \lambda)^{-1} = \begin{bmatrix} I & G(\lambda)a\langle \cdot, a \rangle \\ 0 & I + \lambda G(\lambda)a\langle \cdot, a \rangle \end{bmatrix} (A_0 - \lambda)^{-1}.$$

The range of $(A_0 - \lambda)^{-1}$ is $\text{Dom}(A_0) = H^2(0, \pi) \cap H_0^1(0, \pi) \times H_0^1(0, \pi)$, on which the operator on the left is bounded following lemma 1 and Theorem 1. Splitting up the operator above into an identity plus a second operator and applying the triangle inequality yields

$$\|(A - \lambda)^{-1}\|_{L(X)} \leq \|(A_0 - \lambda)^{-1}\|_{L(X)} \left(1 + \left\| \begin{bmatrix} 0 & G(\lambda)a \langle \cdot, a \rangle \\ 0 & \lambda G(\lambda)a \langle \cdot, a \rangle \end{bmatrix} \right\|_{L(X)} \right).$$

To obtain the norm of the operator on the right, take the supremum over multiplying on the right by all unit vectors $V = [u, v]^T \in X$. It is clear that the supremum will occur with $u = 0$ and thus $\|v\|_{L^2(0, \pi)} = 1$. The function v only acts inside the inner product and so the scalar $\langle v, a \rangle$ may be extracted. Applying these observations yields

$$\frac{\|(A - \lambda)^{-1}\|_{L(X)}}{\|(A_0 - \lambda)^{-1}\|_{L(X)}} = 1 + \sup_{\substack{\|v\|=1 \\ v \in H_0^1(0, \pi)}} |\langle v, a \rangle| \sqrt{\|(G(\lambda)a)'\|^2 + |\lambda|^2 \|G(\lambda)a\|^2}.$$

By analogy with the argument showing $G(0)a \in H_0^1(0, \pi)$ in the proof of Theorem 1 and our explicit form for $G(\lambda)$, one could show $G(\lambda)a \in H_0^1(0, \pi)$. Then using Wirtinger's inequality (Poincaré inequality in one dimension),

$$\|G(\lambda)a\| \leq \|(G(\lambda)a)'\|,$$

resulting in the bound

$$\frac{\|(A - \lambda)^{-1}\|_{L(X)}}{\|(A_0 - \lambda)^{-1}\|_{L(X)}} \leq 1 + \sqrt{1 + |\lambda|^2} \|(G(\lambda)a)'\| \sup_{\substack{\|v\|=1 \\ v \in H_0^1(0, \pi)}} |\langle v, a \rangle|.$$

The scalar $\langle v, a \rangle$ measures the proximity of a to the space $H_0^1(0, \pi)$. When $a \in L^2(0, \pi)$ the choice of v that maximizes $\langle v, a \rangle$ is a scalar multiple of a , and this term obtains its maximum at $\|a\|$. When $a \notin L^2(0, \pi)$, a choice for the optimal v is not apparent, but provided a is singular as defined by (3.11) then by lemma 1 this inner product is bounded.

The resolvent of A_0 may look troublesome, but in fact is explicitly computable. As A_0 is skew-adjoint on X , it is normal, and so by Kato [13, V.3, eq. 3.31],

$$\|(A_0 - \lambda)^{-1}\|_{L(X)} = \sup_{z \in \sigma(A_0)} |z - \lambda|^{-1} = \sup_{n \in \mathbb{Z} \setminus \{0\}} |\lambda - in|^{-1}. \quad (5.4)$$

Thus the final bound on the resolvent of A may be written:

$$\|(A - \lambda)^{-1}\|_{L(X)} \leq \frac{1 + \sqrt{1 + |\lambda|^2} \|(G(\lambda)a)'\| \left(\sup_{\substack{\|v\|=1 \\ v \in H_0^1(0,\pi)}} |\langle v, a \rangle| \right)}{\inf_{n \in \mathbb{Z} \setminus \{0\}} |\lambda - in|}. \quad (5.5)$$

Numerical experiments show this bound is sharp enough to reveal eigenvalue locations. Figure 5.1 illustrates the $\sqrt{1 + |\lambda|^2} \|(G(\lambda)a)'\|$ term in this bound is sufficient to locate eigenvalues when $a(x) = 2/(\pi x)$. This omits the scaling by the resolvent of A_0 , but as the eigenvalues for this operator are not near the imaginary axis, that contribution is irrelevant.

To show that singular functions like $1/x$ have no eigenvalues close to the imaginary axis, one approach is to show that the resolvent is bounded on the imaginary axis. Applying the estimate from Theorem 7 showing that eigenvalues asymptotically move a finite distance away from the imaginary axis will allow the $\|(A_0 - \lambda)^{-1}\|_{L(X)}$ term to be bounded above by a constant, and hence ignored. Then the eigenvalues of A will occur only at poles of $\|(G(\lambda)a)'\|$. However the details of this, and perhaps a proof, await completion.

5.3 Resolvent lower bound

In this section I derive a lower bound on the resolvent. Unlike the bound constructed in section 4.3, this bound is appropriate for singular a . A similar approach will be followed; recall from equation (4.5),

$$\frac{\|\Psi\|_X}{\|(A - \lambda)\Psi\|_X} \leq \|(A - \lambda)^{-1}\|_{L(X)} \quad \forall \Psi \in \text{Dom}(A). \quad (5.6)$$

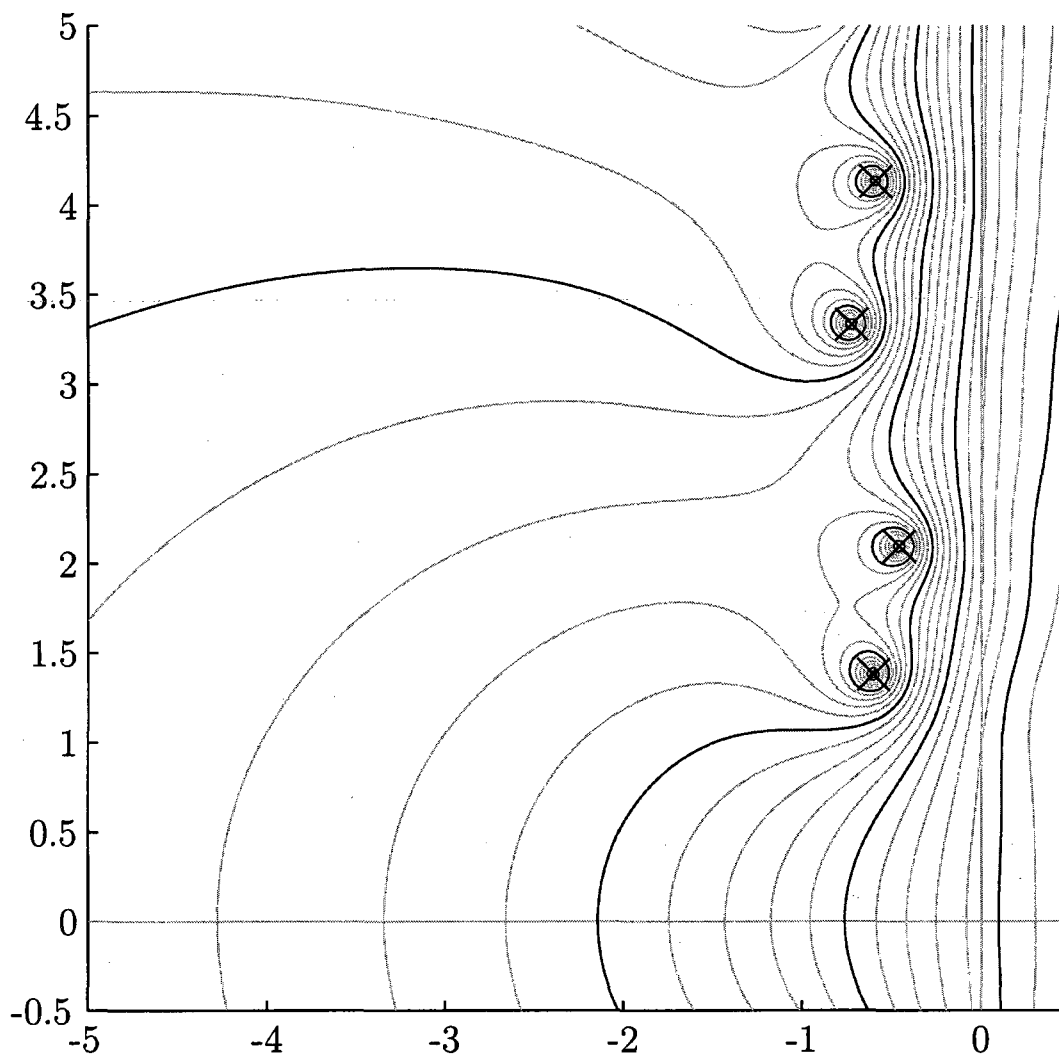


Figure 5.1 : Upper bound on the resolvent for a singular field. Here $a(x) = 2/(\pi x)$. Contours represent the log base ten value of $\sqrt{1 + |\lambda|^2} \|(G(\lambda)a)'\|$. Black contours measure differences of 1 logarithmically, beginning at 1 near the origin and increasing in magnitude towards (numerically computed) eigenvalues, marked with black \times 's. Gray contours are equally spaced, with 5 between each black line. Observe this term alone from equation (5.5) is sufficient to locate eigenvalues in this case.

Construct $\Psi = f[1, \lambda]^T$. Here f will be a mollification of y such that f satisfies $f(0) = f(\pi) = 0$ and *approximately* satisfies the $\mathcal{L}_\lambda y = 0$. The mollification r is constructed such that it is supported only on the interval $[\hat{x}, \pi]$, $r(\pi) = 1$, and $r'(\hat{x}) = 0$. Thus $f = y - y(\pi, \lambda)r$ satisfies the boundary conditions and is a member of $H_0^1(0, \pi)$, but now $\mathcal{L}_\lambda f \neq 0$ if $y(\pi, \lambda) \neq 0$.

There many choices for r . Generally, a quadratic is sufficient; however, the special structure of this problem poses some difficulty. Note that

$$\mathcal{L}_\lambda f = 0 + y(\pi, \lambda)\mathcal{L}_\lambda r = y(\pi, \lambda) (r'' - \lambda^2 r - \lambda a \langle r, a \rangle), \quad (5.7)$$

so if $\langle r, a \rangle \neq 0$ and $a \notin L^2(0, \pi)$ then the norm of $\mathcal{L}_\lambda f$ could be unbounded if $\langle r, a \rangle \neq 0$ and $a \notin L^2(0, \pi)$. Thus r should be built orthogonal to a . To construct such an r , define

$$q(x) = \begin{cases} 0, & x \in [0, \hat{x}]; \\ (x - \hat{x})/(\pi - \hat{x}), & x \in (\hat{x}, \pi]. \end{cases}$$

Then r is formed as a linear combination of q^2 and q^3 that is orthogonal to a . The choice

$$r(x) = \alpha q^2(x) - \beta q^3(x) \quad (5.8)$$

with

$$\alpha = \frac{\langle q^3, a \rangle - 1}{\langle q^3, a \rangle - \langle q^2, a \rangle} \quad \beta = \frac{\langle q^2, a \rangle - 1}{\langle q^3, a \rangle - \langle q^2, a \rangle}$$

satisfy the required conditions such that r is a mollification and ensures $\langle r, a \rangle = 0$. Should α or β diverge or go to zero, a different choice of \hat{x} should suffice to construct an appropriate mollification.

Unfortunately, due to the complexity of $y(x, \lambda)$ and r , there is no obvious choice of \hat{x} or a simple form of the resolvent bound generated by this choice of f . Computationally, this bound does reasonably well, as shown in figure 5.2.

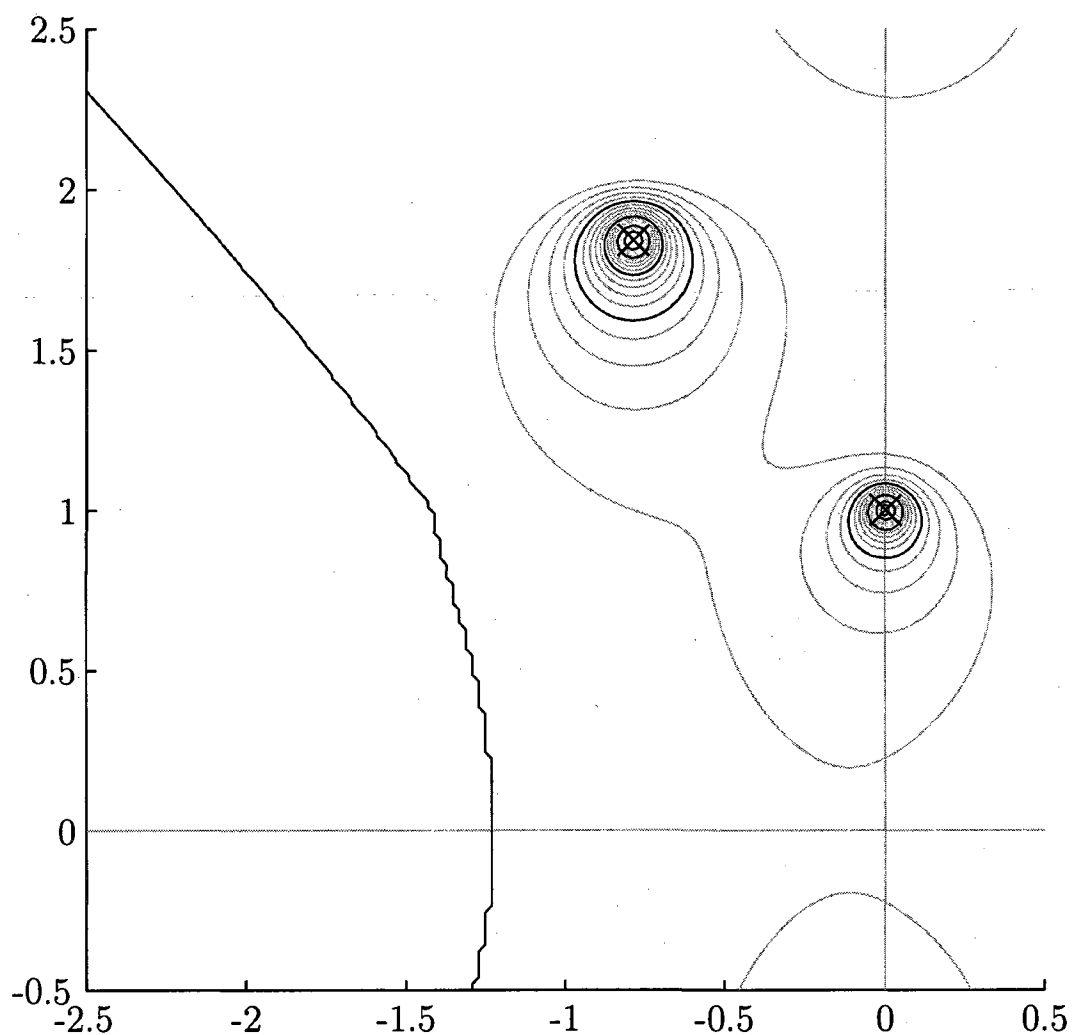


Figure 5.2 : Mollification lower bound on the resolvent. Here $a(x) = \sin(2x)$. The gray and black lines are contours of the log base ten of the lower bound given by the mollification (5.8). Black contours indicate differences of $1/4$, starting from 0 and increasing towards the black \times 's. These black \times 's denote exact eigenvalues (see equation (4.11)); hence this lower bound accurately locates eigenvalues. Spectral methods are used to construct y and its derivative, as described in Appendix B.

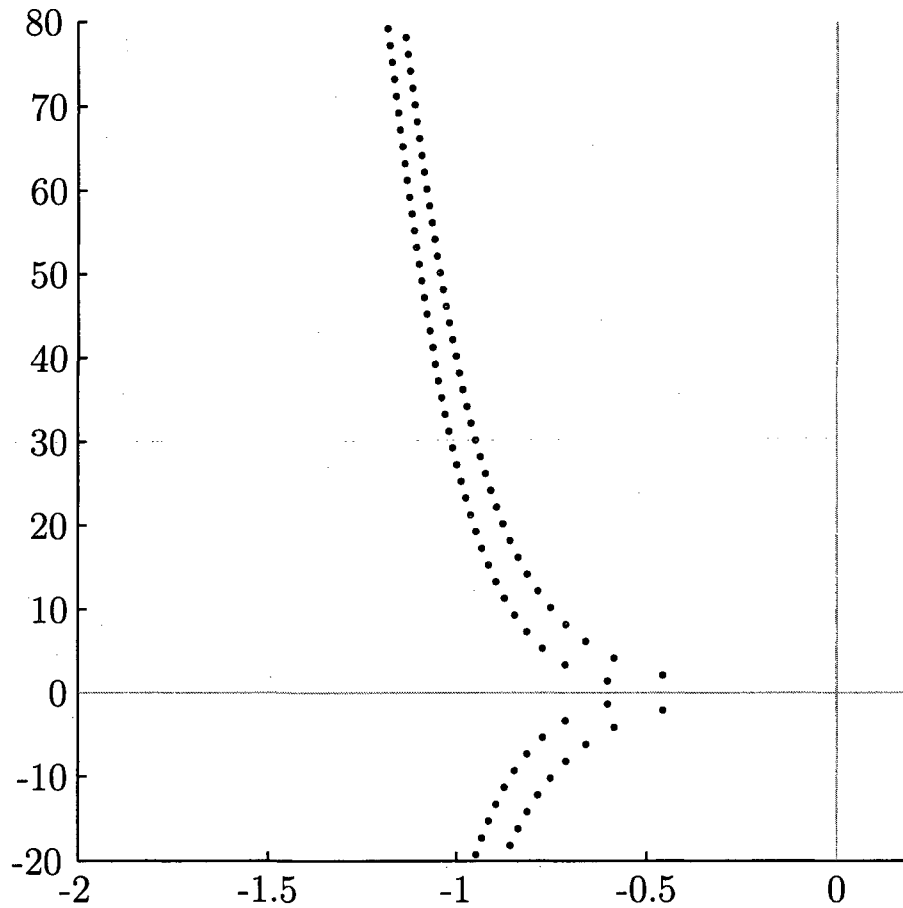


Figure 5.3 : Spectrum of A when $a(x) = 2/(\pi x)$. Here, $\sigma(A)$ was computed with a discretization of dimension $N = 2048$ as described in Appendix B.

5.4 Is $a(x) = \gamma/x$ optimal?

Although the numerics and the rate of eigenvalues leaving the imaginary axis both suggest that $a(x) = \gamma/x$ makes the spectral abscissa negative, it is not clear that $a(x) = \gamma/x$ moves the eigenvalues uniformly off the axis, as the Castro–Cox function does. In the high frequency limit, eigenvalues for $a(x) = \gamma/x$ are uniformly negative as $\gamma \rightarrow 2/\pi$. The low frequency eigenvalues display a complicated structure as see in figure 5.3. This suggests that by perturbing $a(x)$, a function can be found that moves

Table 5.2 : Numerically optimal finite Laurent series. A spectral discretization of A is constructed of size 1024 and an estimate of the spectral abscissa based on low frequency eigenvalues is optimized using MATLAB's `fminsearch` optimization routine. The exact coefficients are sensitive to the initial condition, but the abscissa generated is stable.

| Terms | Abscissa | γ_{-1} | γ_0 | γ_1 | γ_2 |
|-------|----------|---------------|------------|------------|------------|
| 1 | -0.48799 | 0.65027 | | | |
| 2 | -0.68366 | 0.63069 | 0.03899 | | |
| 3 | -0.65403 | 0.63841 | 0.01160 | 0.01729 | |
| 4 | -0.65131 | 0.63874 | 0.01148 | 0.01618 | 0.00070 |

the spectrum uniformly.

One approach is to expand the hypothetical function in terms of a Laurent series,

$$a(x) = \sum_{j=-1}^{\infty} \gamma_j x^j.$$

Running an optimization routine on this function to minimize the spectral abscissa with a finite number of terms in the series results in a smaller spectral abscissa numerically, as shown in Table 5.2. This approach is similar to Freitas [10]; however, I cannot claim to have found a ‘better’ damping function without further work. This optimization approach does not suggest a simple form for a better function — I have been unable to find a series for a well-known function that resembles the coefficients in Table 5.2. This is not surprising due to the sensitivity of the coefficients γ_j to changes in discretization size and starting values for the optimization routine. A superior damping function to $a(x) = \gamma/x$ might exist, but further investigation is needed.

Chapter 6

Conclusions

I have studied a family of damped wave operators parametrized by a function $a(x) : [0, \pi] \rightarrow \mathbb{R}$. These operators correspond to the magnetic damping of an elastic conductor in which a is proportional to the magnetic field strength. My objective in studying this operator was to find those choices of a that lead to energy decay. Similar questions have already been asked of the related Kelvin–Voigt and viscous damping operators, as described in Chapter 2. Theorem 4 reveals, when $a \in BV(0, \pi)$, that the energy decay is bounded by the spectral abscissa, which, as Theorem 3 showed, is zero. Thus for any time $T > 0$ there exist initial conditions such that arbitrarily little energy is lost over $t \in [0, T]$.

This lack of decay in the bounded variation case motivated the study of singular fields in Chapter 5. Theorem 7 provides a suggestion that all eigenvalues of A might move off the imaginary axis. Numerical examples were then presented confirming this result. In this chapter I also established two bounds on the resolvent: one lower (section 5.3), one upper (section 5.2). The structure of each bound is complicated, but could provide an avenue for future work on this operator. The combination of these two bounds should enable localization eigenvalues of A by finding the intersection where both bounds diverge. However, the upper bound alone would also be useful in establishing where eigenvalues of A may reside. Alternatively, Rouché type analysis could be applied to the shooting function $y(\pi, \lambda)$ to bound the location of eigenvalues, in a similar manner to Theorem 3, but now strictly away from the imaginary axis.

Additional work will also be required to ensure that the spectral abscissa governs the rate of decay in the singular case. When a is singular, $a\langle \cdot, a \rangle$ is no longer a bounded perturbation to a skew-adjoint operator, and so more sophisticated techniques will be required to establish that the eigenvectors of A form a Riesz basis.

It is my belief that this operator will eventually yield to analysis that will confirm the case $a(x) = 2/(\pi x)$ does indeed move all eigenvalues finitely off the imaginary axis. What is less clear is whether the efficacy of this improved spectral abscissa is tempered by large resolvent norms near the imaginary axis.

Appendix A

Derivation of Magnetic Damping

This appendix contains a derivation of the equations of motion for a conductive string in a magnetic field, as seen in equation (1.1). Two levels of sophistication are generally used for such derivations. One begins with an equilibrium state and assumes small perturbations to this equilibrium. These are commonly seen in physics textbooks and justly chastised by Antman [2, p. 13]. The proper approach is a derivation beginning at three dimensional nonlinear elasticity following Antman [2, ch. 2]. In the case of a constant magnetic field, a derivation of this type was completed by Wolfe [24, §2]; the case of non-constant field will be covered in an upcoming paper [8]. These derivations and subsequent linearizations, although the correct approach, mask the underlying physical processes in their sophistication. In this appendix, I seek a balance between these two extremes. I begin with the linearized wave equation with an additional forcing term, and then show this forcing term is the perturbation in the equation of motion for a magnetically damped string.

To begin, consider a string with constant tension σ and constant linear density ρ . The linear equation of motion for this string with an additional force $\mathbf{F}(x, t)$ acting pointwise is

$$\rho \frac{\partial^2 u}{\partial t^2}(x, t) = \sigma \frac{\partial^2 u}{\partial x^2}(x, t) + \mathbf{F}(x, t) \cdot \hat{\mathbf{y}}, \quad (\text{A.1})$$

where $\hat{\mathbf{y}}$ is the unit vector perpendicular to the string's rest state. In the case of magnetic damping, $\mathbf{F}(x, t)$ depends on $u(x, t)$ as illustrated below.

Define the surface $S(t)$ to be the manifold in the $\hat{\mathbf{x}}, \hat{\mathbf{y}}$ plane bounded by $u(x, t)$ and

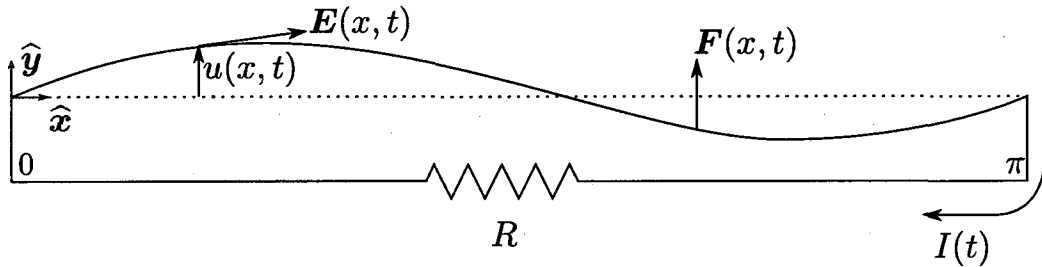


Figure A.1 : Physical setting for magnetic damping. An elastic conductive string is stretched between two rigid endpoints a length π apart. The two ends of the string are connected through a resistor R . A magnetic field $\mathbf{B}(x)$ permeates the region from the \hat{z} direction (out of page). As the string is displaced, $u(x, t)$, it induces an electromotive force $\mathbf{E}(x, t)$. This electromotive force induces a current $I(t)$ through the resistor R . A Lorentz force $\mathbf{F}(x, t)$ then acts on the string.

Table A.1 : Variables required for derivation of magnetic damping equations of motion

| | |
|---|---|
| x, y, z | coordinates relative to axes in figure A.1 |
| $\hat{x}, \hat{y}, \hat{z}$ | right handed unit vectors for \mathbb{R}^3 as labeled in figure A.1 |
| $\mathbf{x} = [x, y, z]$ | vectorized form of above |
| σ | tension in string |
| ρ | linear mass density of string |
| R | resistance through current loop |
| $I(t)$ | current in string loop |
| $u(x, t)$ | string displacement |
| $\mathbf{E}(x, t)$ | electric field induced in loop at x |
| $\mathbf{F}(x, t)$ | force acting on the string |
| $\mathbf{B}(\mathbf{x}, t) = B(x)\hat{z}$ | external magnetic field |

the current return path illustrated in figure A.1. Additionally, let S_0 be similarly defined when $u(x, t) \equiv 0$. As the string traverses the external magnetic field, it encloses a variable amount of the magnetic flux. Then using Faraday's law of induction [12, eq. 7.15]

$$\oint_{\partial S(t)} \mathbf{E} \cdot d\boldsymbol{\ell} = -\frac{\partial}{\partial t} \iint_{S(t)} \mathbf{B} \cdot d\mathbf{a}.$$

To take the derivative over this time-changing surface, note that the integral over $S(t)$ may be composed of S_0 and an additional surface:

$$\begin{aligned} \oint_{\partial S(t)} \mathbf{E} \cdot d\boldsymbol{\ell} &= -\frac{\partial}{\partial t} \left(\iint_{S_0} \mathbf{B} \cdot d\mathbf{a} + \int_0^\pi \int_0^{u(x,t)} \mathbf{B}([x, y, 0]) \cdot \hat{\mathbf{z}} dy dx \right) \\ &= -\frac{\partial}{\partial t} \int_0^\pi (u(x, t)) B(x) dx \\ &= -\int_0^\pi \frac{\partial u}{\partial t}(x, t) B(x) dx. \end{aligned} \tag{A.2}$$

If vibrations of $u(x, t)$ are sufficiently slow, a uniform current will be established in the loop. As the current reaches equilibrium on a time scale of the length of the string times the speed of light, for physical vibrations, this assumption is warranted. The current may be calculated from the electromotive force in equation (A.2) via Ohm's law and flipping signs, as $\partial S(t)$ and $I(t)$ are oriented in opposite directions. This yields

$$I(t) = -\frac{1}{R} \oint_{\partial S} \mathbf{E} \cdot d\boldsymbol{\ell}. \tag{A.3}$$

The current flowing inside the string interacts with the surrounding magnetic field through a Lorentz force [12, eq. 5.16]. At each point x the current flows parallel with the string, and in this linearization the angles of displacement are assumed small; then the current flows effectively in the $\hat{\mathbf{x}}$ direction. Hence,

$$\mathbf{F}(x, t) = [I(t)\hat{\mathbf{x}}] \times [B(x)\hat{\mathbf{z}}] = -B(x)I(t)\hat{\mathbf{y}} \tag{A.4}$$

in the limit of small vibrations. So finally, the forcing term may be written as

$$\mathbf{F}(x, t) = -\frac{B(x)}{R} \int_0^\pi \frac{\partial u}{\partial t}(\xi, t) B(\xi) d\xi \hat{\mathbf{y}}. \quad (\text{A.5})$$

Setting $a(x) = B(x)/\sqrt{R}$ and $\rho = \sigma = 1$, the partial differential equation for the string with magnetic damping, equation (1.1), is obtained.

Appendix B

Spectral Methods

Numerical experiments have been used throughout my research to provide intuition about the magnetic damping operator. A wide variety of techniques can be used to approximate the magnetic damping operator, but I have chosen to primarily use Chebyshev pseudospectral collocation methods as described by Trefethen [21]. These methods approximate derivatives and integrals by exactly differentiating and integrating interpolants to those functions on a Chebyshev grid. The resulting differentiation matrices are dense, unlike lower order finite difference methods, increasing computational cost. Unlike lower order methods, however, this method will converge exponentially as the discretization size is increased for smooth functions. For damped wave problems, the solutions are smooth for most a , so this spectral method will perform well. Below, I will describe how this spectral method may be applied to the magnetic damping problem.

B.1 Chebyshev differentiation matrices

Regularly spaced grids are a poor basis on which to approximate derivatives with a high degree of accuracy due to Runge's phenomenon. Grids with points clustered near the boundaries turn out to be superior in most cases; Chebyshev points are one example of such a grid. For a discretization size N , Chebyshev points on $(-1, 1)$

are [21, eq. 5.2]

$$x_j = \cos(j\pi/N). \quad (\text{B.1})$$

The function $f(x)$ is approximated on this grid by constructing the vector \mathbf{f} where

$$[\mathbf{f}]_j = f(x_j)$$

samples f at the grid points $\mathbf{x} = (x_0, x_1, \dots, x_{N+1})^T$. Similarly, define \mathbf{f}' as $f'(x)$ evaluated at grid points. Then a differentiation matrix $\mathbf{D} \in \mathbb{C}^{(N+1) \times (N+1)}$ may be constructed such that $\mathbf{D}\mathbf{f} \approx \mathbf{f}'$ following [21, eq. 6.3–5]. This matrix \mathbf{D} is dense, making computations expensive, but if f is smooth, then as $N \rightarrow \infty$, the error in the approximation decays exponentially.

B.2 Approximating the undamped wave operator

The undamped wave operator is approximated by using the approximate derivative operator \mathbf{D} . The resulting approximation mimics the structure of (2.3). First, though, the second derivative operator needs to be approximated. Simply squaring the derivative operator, \mathbf{D} , on the Chebyshev grid is sufficient for this purpose. To enforce the Dirichlet boundary conditions, observe that the first and last entries in \mathbf{f} and $\mathbf{D}^2\mathbf{f}$ must be zero. Thus the first and last columns and first and last rows of \mathbf{D}^2 are removed, leaving $\mathbf{L} \in \mathbb{C}^{(N-1) \times (N-1)}$ [21, p. 62].

Now the undamped wave operator on $(0, \pi)$ may be formed by scaling \mathbf{x} and \mathbf{L} appropriately for this domain. Namely,

$$\begin{aligned} (\pi/2)(\mathbf{x} - 1) &\rightarrow \mathbf{x}, \\ (2/\pi)^2\mathbf{L} &\rightarrow \mathbf{L}. \end{aligned}$$

Table B.1 : Convergence of spectral methods for the undamped wave operator. This table compares eigenvalues of the true operator to eigenvalues of the approximation on grids of size 8 and 16. As this illustrates, the first $N/2$ eigenvalues are accurate; a feature seen repeatedly in practice. The conjugate pairs of these eigenvalues have been omitted, but share the same error properties.

| Exact | $N = 8$ | $N = 16$ |
|-------|---------------------|---------------------|
| $1i$ | $0.99999997711157i$ | $1.00000000000000i$ |
| $2i$ | $2.00004618424119i$ | $2.00000000000087i$ |
| $3i$ | $2.99856926441649i$ | $3.00000000021948i$ |
| $4i$ | $4.05271176596448i$ | $3.9999993203235i$ |
| $5i$ | $4.72021971131075i$ | $4.9999871401721i$ |
| $6i$ | $9.03919773621486i$ | $6.00004061504667i$ |
| $7i$ | $9.32104180081907i$ | $6.99955182665405i$ |

Forming the matrix $A \in \mathbb{C}^{2(N-1) \times 2(N-1)}$ where

$$A = \begin{bmatrix} \mathbf{0} & \mathbf{I} \\ \mathbf{L} & \mathbf{0} \end{bmatrix}, \quad (\text{B.2})$$

and \mathbf{I} is the $(N-1) \times (N-1)$ identity matrix, this A approximates the undamped wave operator.

The eigenvalues for the undamped wave equation are simply the integers times i excepting 0. The Chebyshev spectral approximation of A , denoted \mathbf{A} , approximates these eigenvalues well even for small N , as seen in Table B.1. Code to construct this matrix is shown in figure B.1. The routine `cheb.m` is Trefethen's code for constructing Chebyshev differentiation matrices, described in [21], and is available online at <http://web.comlab.ox.ac.uk/nick.trefethen/spectral.html>.

```

N = 16;
[D,x] = cheb(N);
L = D^2;
L = L(2:N,2:N);
L = L*(2/pi)^2;
A = [zeros(N-1) eye(N-1); L zeros(N-1)];

```

Figure B.1 : Code generating an approximation of the undamped wave operator.

B.3 Approximating the magnetic damping operator

The magnetic damping operator differs from the undamped wave operator by a rank-1 perturbation in the (2,2) block. Similarly, the discretization of this operator will differ from the undamped discretization by a rank-1 perturbation.

We now need to approximate the operator $a\langle \cdot, a \rangle$, i.e., we want to construct a matrix C so that when the vector \mathbf{f} samples the function f on the Chebyshev grid, then $C\mathbf{f} \approx a\langle f, a \rangle$. This clearly requires an approximation of the integral in the inner product. Since \mathbf{f} is represented at Chebyshev points, it is natural to use Clenshaw–Curtis quadrature, a high-order quadrature rule based on exactly integrating the polynomial interpolant to a function at Chebyshev points. Let the vector \mathbf{w} represent the quadrature weights for the $N+1$ point Clenshaw–Curtis rule. Then the integration $\int_0^\pi f(x) dx$ may be approximated by the inner product $\mathbf{w}^T \mathbf{f}$. To construct damping term in the magnetic damping operator, first the integral $\langle \cdot, a \rangle$ must be constructed. Denote pointwise vector multiplication by the symbol \odot . Then for some vector \mathbf{f} ,

$$\langle \mathbf{f}, a \rangle \approx \mathbf{w}^T (\mathbf{f} \odot \mathbf{a}) = (\mathbf{w} \odot \mathbf{a})^T \mathbf{f}. \quad (\text{B.3})$$

In a similar manner, the action of the operator $a\langle \cdot, a \rangle$ is approximated by the outer

product

$$a\langle \cdot, a \rangle \approx a(w \odot a)^T. \quad (\text{B.4})$$

Using this approximation for the damping, the wave operator may be approximated by

$$\mathbf{A} = \begin{bmatrix} \mathbf{0} & \mathbf{I} \\ \mathbf{L} & -a(w \odot a)^T \end{bmatrix}. \quad (\text{B.5})$$

The code for constructing this \mathbf{A} shown in figure B.2 differs from the undamped wave code only in the change of the (2,2) block. When a is smooth, this method works well, as demonstrated in Table B.2. When a is singular, this method converges slowly. Grids of size 1024 or larger are needed to resolve low frequency eigenvalues to reasonable precision, as shown in table B.3. Better numerical approaches are needed here.

Spectral methods and Clenshaw–Curtis quadrature are also used in several other areas of this thesis. They are used to construct the shooting functions y and w , along with $G(\lambda)a$, used in sections 5.2 and 5.3. Building approximations to these objects follows simply from their respective definitions.

```

a = @(x) sqrt(2)*sqrt(2/pi)*sin(1*x);
N = 16;
% Construct differentiation matrix
[D,x] = cheb(N);
L = D^2;
L = L(2:N,2:N);
L = L*(2/pi)^2;
% Construct damping term
[x,w] = clencurt(N);
x = pi/2*(1+x(2:N)); w = pi/2*w(2:N);
ax = a(x);
C = ax*(w.*ax');
A = [zeros(N-1) eye(N-1); L -C];

```

Figure B.2 : Code generating an approximation of the magnetic damping operator.

Table B.2 : Eigenvalue convergence for spectral approximation of the magnetic damping operator when $a \in BV(0, \pi)$. Specifically $a(x) \equiv 0.8$. Convergence follows a similar pattern to Table B.1. Note that even eigenvalues (those approximating $2in$ for $n \in \mathbb{Z}^+$) are undamped, as predicted by Theorem 3.

| $N = 16$ | $N = 256$ |
|--|---|
| $-0.84597839166559 + 0.56481991443707i$ | $-0.84597839166538 + 0.56481991444776i$ |
| $-0.00000000000000 + 2.000000000000087i$ | $-0.000000000000004 + 1.999999999999452i$ |
| $-0.06588872814612 + 2.95834400444970i$ | $-0.06588872808362 + 2.95834400428002i$ |
| $-0.00000000000000 + 3.99999993203234i$ | $0.000000000000003 + 4.000000000000070i$ |
| $-0.02834893734824 + 4.98890387449988i$ | $-0.02834904174222 + 4.98890511896678i$ |
| $0.000000000000001 + 6.00004061504667i$ | $0.00000000000000 + 5.99999999999974i$ |
| $-0.01538451336862 + 6.99519928607148i$ | $-0.01541014475877 + 6.99563975558354i$ |

Table B.3 : Eigenvalue convergence for spectral approximation of the magnetic damping operator when $a(x) = 2/(\pi x)$. Note that convergence is far slower than seen previously in Tables B.1 and B.2.

| $N = 256$ | $N = 1024$ |
|---|---|
| $-0.60324627212638 + 1.37890054767696i$ | $-0.60254808326093 + 1.37924089900725i$ |
| $-0.45749313204658 + 2.10066302903099i$ | $-0.45708144585507 + 2.10135242862779i$ |
| $-0.71758009884126 + 3.33459474744582i$ | $-0.71423043875790 + 3.33545485745885i$ |
| $-0.58744884573420 + 4.14090611536783i$ | $-0.58521736451053 + 4.14301600389049i$ |
| $-0.78205632165110 + 5.31619430194206i$ | $-0.77423682058696 + 5.31780556506505i$ |
| $-0.66553939907565 + 6.15881104985526i$ | $-0.66008418625021 + 6.16288854260860i$ |
| $-0.83036927072012 + 7.30520777330564i$ | $-0.81623925765204 + 7.30790060104027i$ |

Bibliography

- [1] M. ABRAMOWITZ AND I. A. STEGUN, *Handbook of Mathematical Functions with Formulas, Graphs, and Mathematical Tables*, U.S. Department of Commerce, 1964.
- [2] S. S. ANTMAN, *Nonlinear Problems of Elasticity*, Springer, New York, second ed., 2005.
- [3] G. K. BATCHELOR, *An Introduction to Fluid Dynamics*, Cambridge University Press, 2000.
- [4] H. BREZIS, *Analyse Fonctionnelle: Théorie et Applications*, Masson, Paris, second ed., 1993.
- [5] C. CASTRO AND S. J. COX, *Achieving arbitrarily large decay in the damped wave equation*, SIAM J. Control Optim., 39 (2001), pp. 1748–1755.
- [6] S. CHEN, K. LIU, AND Z. LIU, *Spectrum and stability for elastic systems with global or local Kelvin-Voigt damping*, SIAM J. Appl. Math., 59 (1999), pp. 651–668.
- [7] S. COX AND E. ZUAZUA, *The rate at which energy decays in a damped string*, Comm. Partial Differential Equations, 19 (1994), pp. 213–243.
- [8] S. J. COX, M. EMBREE, J. M. HOKANSON, AND W. A. KELM, *Magnetic damping of an elastic conductor*. In preparation.
- [9] S. J. COX AND M. L. OVERTON, *Perturbing the critically damped wave equation*, SIAM J. Appl. Math., 56 (1996), pp. 1353–1362.
- [10] P. FREITAS, *Optimizing the rate of decay of solutions of the wave equation using genetic algorithms: a counterexample to the constant damping conjecture*, SIAM J. Control Optim., 37 (1999), pp. 376–387.
- [11] I. C. GOHBERG AND M. G. KREĬN, *Introduction to the Theory of Linear Non-selfadjoint Operators*, American Mathematical Society, Providence, R.I., 1969.
- [12] D. J. GRIFFITHS, *Introduction to Electrodynamics*, Prentice-Hall, London, third ed., 1999.

- [13] T. KATO, *Perturbation Theory for Linear Operators*, Springer-Verlag, Berlin, 1995. Reprint of the 1980 edition.
- [14] M. A. LEIBOWITZ AND R. C. ACKERBERG, *The vibration of a conducting wire in a magnetic field*, Quart. J. Mech. Appl. Math., 16 (1963), pp. 507–519.
- [15] S. P. LIN, *Damped vibration of a string*, J. Fluid Mech., (1975), pp. 787–797.
- [16] K. LIU AND Z. LIU, *Exponential decay of energy of vibrating strings with local viscoelasticity*, Z. Angew. Math. Phys., 53 (2002), pp. 265–280.
- [17] M. A. PINSKY, *Introduction to Fourier Analysis and Wavelets*, Brooks/Cole, Pacific Grove, CA, 2002.
- [18] M. REED AND B. SIMON, *Functional Analysis*, Academic Press, San Diego, 1980.
- [19] M. RENARDY, *On localized Kelvin-Voigt damping*, Z. Angew. Math. Mech., 84 (2004), pp. 280–283.
- [20] W. RUDIN, *Principles of Mathematical Analysis*, McGraw-Hill, New York, third ed., 1976.
- [21] L. N. TREFETHEN, *Spectral Methods in MATLAB*, Society for Industrial and Applied Mathematics (SIAM), Philadelphia, PA, 2000.
- [22] L. N. TREFETHEN AND M. EMBREE, *Spectra and Pseudospectra: The Behavior of Nonnormal Matrices and Operators*, Princeton University Press, Princeton, NJ, 2005.
- [23] C. TRUESDELL, *The Rational Mechanics of Flexible or Elastic Bodies, 1638–1788*, Leonhardi Euleri Opera Omnia, Series secunda (Opera mechanica et astronoca), Vol. XI, sectio secunda. Auctoritate et impensis Societatis Scientiarum Naturalium Helveticae, Orell Füssli, Zürich, 1960.
- [24] P. WOLFE, *Small vibrations of an elastic conductor in a magnetic field*, Math. Methods Appl. Sci., 21 (1998), pp. 1559–1569.